Dicarboxylic acids, oxoacids, benzoic acid, α-dicarbonyls, WSOC, OC, and ions in spring aerosols from Okinawa Island in the western North Pacific Rim: Size distributions and formation processes

D. K. Deshmukh[1,2], K. Kawamura[1,2]*, M. Lazaar[1,3], B. Kunwar[1], and S. K. R. Boreddy[1]

[1] Institute of Low Temperature Science, Hokkaido University, Sapporo 060-0819, Japan

[2] Now at Chubu Institute for Advanced Studies, Chubu University, Kasugai 487-8501, Japan

[3] Ecole National Supérieure de Chimie de Rennes (ENSCR), Rennes 35708, France

*Corresponding author

E-mail address: kkawamura@isc.chubu.ac.jp

Abstract

Size-segregated aerosols (9-stages from <0.43 to >11.3 μm in diameter) were collected at Cape Hedo, Okinawa in spring 2008 and analyzed for water-soluble diacids (C_2-C_{12}), ω-oxoacids (ωC_2-ωC_9), pyruvic acid, benzoic acid and α-dicarbonyls (C_2-C_3) as well as water-soluble organic carbon (WSOC), organic carbon (OC) and major ions (Na^+, NH_4^+, K^+, Mg^{2+}, Ca^{2+}, Cl^-, NO_3^-, SO_4^{2-}, and MSA^-). In all the size-segregated aerosols, oxalic acid (C_2) was found as the most abundant species followed by malonic and succinic acids whereas glyoxylic acid (ωC_2) was the dominant oxoacid and glyoxal (Gly) was more abundant than methylglyoxal. Diacids (C_2-C_5), ωC_2 and Gly as well as WSOC and OC peaked at fine mode (0.65-1.1 μm) whereas azelaic (C_9) and 9-oxononanoic (ωC_9) acids peaked at coarse mode (3.3-4.7 μm). Sulfate and ammonium were enriched in fine mode whereas sodium and chloride were in coarse mode. Strong correlations of C_2-C_5 diacids, ωC_2 and Gly with sulfate were observed in fine mode (r = 0.86-0.99), indicating a commonality in their secondary formation. Their significant correlations with liquid water content in fine mode (r = 0.82-0.95) further suggest an importance of the aqueous-phase production in Okinawa aerosols. They may also have been directly emitted from biomass burning in fine mode as supported by strong correlations with potassium (r = 0.85-0.96), which is a tracer of biomass burning. Bimodal size distributions of longer-chain diacid (C_9) and oxoacid (ωC_9) with a major peak in the coarse mode suggest that they were emitted from the sea surface microlayers and/or produced by heterogeneous oxidation of biogenic unsaturated fatty acids on sea salt particles.

Keywords: Water-soluble organic species, ions, size-segregated aerosols, unimodal distribution, bimodal distribution, secondary aerosols.

1 Introduction

Tropospheric aerosol is an important environmental issue because it dramatically reduces the visibility (Jacobson et al., 2000; Kanakidou et al., 2005), affects the radiative forcing of climate (Seinfeld and Pandis, 1998), and causes a negative impact on human health (Pope and Dockery, 2006). All of these effects strongly depend on the abundances of aerosols and their chemical and physical properties in different sizes. Particles in diameter of 0.1-1.0 μm are very active in scattering and absorbing incoming solar radiation and have a direct impact on climate (Ramanathan et al., 2001; Seinfeld and Pankow, 2003). The knowledge of size distributions of chemical components is thus essential to better understand their potential contributions to climate change and pollution control. Their size distribution also provides evidences for the sources and formation pathways of atmospheric particles.

The emission sources and multiple secondary formation pathways of organic aerosols are not well understood. Organic compounds account for up to 70% of fine aerosol mass and potentially control the physicochemical properties of aerosol particles (Davidson et al., 2005; Kanakidou et al., 2005). Low-molecular-weight diacids are one of the most abundant organic compound classes in the atmosphere (Kawamura and Ikushima, 1993; Kawamura et al., 1996; Kawamura and Bikkina, 2016). They are primarily derived from incomplete combustion of fossil fuel and biomass burning (Kawamura and Kaplan, 1987; Falkovich et al., 2005), and secondarily produced in the atmosphere via photooxidation of unsaturated fatty acids and volatile organic compounds (VOCs) from biogenic and anthropogenic sources (Kawamura and Gagosian, 1987; Kawamura et al., 1996; Sempéré and Kawamura, 2003). The ability of organic aerosols to act as cloud condensation nuclei (CCN) seems to be closely related to their mass-based size distributions (Pradeep Kumar et al., 2003; Ervens et al., 2007).

The increasing atmospheric burden of organic aerosols is associated with natural and anthropogenic emissions in the continental regions. Organic aerosols are eventually transported to the oceanic regions. The rapid industrialization in East Asia is expected to have important impact on global atmospheric chemistry over the next decades (Wang et al., 2013; Tao et al., 2013; Bian et al., 2014). Large amounts of coal and biomass burning in East Asia add more anthropogenic

aerosols altering the aerosol chemical composition in the remote Pacific atmosphere (Mochida et al., 2007; Miyazaki et al., 2010; Agarwal et al., 2010; Wang et al., 2011; Engling et al., 2013). Water-soluble diacids and related compounds as well as major ions are previously studied for their size distributions in remote marine aerosols (Kawamura et al., 2007: Mochida et al., 2007; Miyazaki et al., 2010), whereas their size-segregated characteristics have not been studied in the western North Pacific Rim.

We collected size-segregated aerosol samples with 9-size ranges in spring 2008 in Cape Hedo, Okinawa in the western North Pacific Rim. Cape Hedo is located on the northern edge of Okinawa Island and can serve as a suitable site for the observation of atmospheric transport of East Asian aerosols with insignificant interference from local emission sources (Takami et al., 2007). The samples were analyzed for dicarboxylic acids (C_2-C_{12}) and related compounds such as ω-oxoacids (ωC_2-ωC_9), pyruvic acid (C_3), and α-dicarbonyls (C_2-C_3) to better understand the sources and processing of water-soluble organic compounds at this marine receptor site. Size-segregated samples were also analyzed for water-soluble organic carbon (WSOC), organic carbon (OC), and major inorganic ions. The role of liquid water content of aerosol in the size distribution of diacids and related compounds is discussed. The potential factors responsible for their size distributions are also discussed.

2 Materials and method

2.1 Site description and aerosol collection

The geographical location of Okinawa Island (26.87°N and 128.25°E) and its surroundings in East Asia are shown in Figure 1. Okinawa is located in the outflow region of continental aerosols and on the pathways to the Pacific. Cape Hedo has been used as a supersite of Atmospheric Brown Clouds project to study the atmospheric transport of Chinese aerosols and their chemical transformation during long-range transport from East Asia (Takiguchi et al., 2008; Kunwar and Kawamura, 2014). The sampling site at Cape Hedo is about 60 m a.s.l.

Size-segregated aerosol samples were collected at Cape Hedo Atmospheric and Aerosol Monitoring Station (CHAAMS) in March 18 to April 13, 2008. This period is characterized by the

86 westerly wind in the lower troposphere, which is the principal process responsible for the transport
87 of both fossil fuel combustion and biomass burning aerosols in East Asia to the western North
88 Pacific. 9-Stage Andersen Middle Volume Impactor (Tokyo Dylec Company, Japan; 100 L min^{-1})
89 was used for the collection of size-segregated samples. The sampler was equipped with quartz fiber
90 filters (QFF, 80 mm in diameter) that were pre-combusted at 450°C for 6 h in a furnace to eliminate
91 the adsorbed organic compounds. A total of five sets (OKI-1 to OKI-5) of size-segregated aerosol
92 samples were collected. Each sample set consists of nine filters for the sizes of <0.43, 0.43-0.65,
93 0.65-1.1, 1.1-2.1, 2.1-3.3, 3.3-4.7, 4.7-7.0, 7.0-11.3, and >11.3 μm. The filter was placed in a
94 preheated 50 mL glass vial with a Teflon-lined screw cap and stored in a freezer at the station. The
95 samples were stored in darkness at -20°C prior to analysis in Sapporo. One set of field blank was
96 collected by placing a pre-combusted QFF for 30s without sucking air before installing real QFF
97 into the sampler.

98 **2.2 Analytical procedures**

99 Diacids and related compounds were determined by the method of Kawamura and Ikushima (1993),
100 and Kawamura (1993). Aliquot of the filters was extracted with organic-free ultrapure water
101 (specific resistivity >18.2 MΩ-cm) under ultrasonication. The extracts were passed through a glass
102 column packed with quartz wool to remove insoluble particles and filter debris. The extracts were
103 concentrated using a rotary evaporator under vacuum and derivatized to dibutyl esters and dibutoxy
104 acetals with 14% BF_3 in *n*-butanol at 100°C. Acetonitrile and *n*-hexane were added into the
105 derivatized sample and washed with organic-free pure water. The hexane layer was further
106 concentrated using a rotary evaporator under vacuum and dried to almost dryness by N_2 blowdown
107 and dissolved in 100 μL of *n*-hexane. Two μL of the sample were injected into a capillary GC
108 (Hewlett-Packard HP6890) equipped with an FID detector. Authentic diacid dibutyl esters were
109 used as external standards for the peak identification and quantification. Identifications of diacids
110 and related compounds were confirmed by GC-mass spectrometry. Recoveries of authentic
111 standards spiked to a pre-combusted QFF were 85% for oxalic acid (C_2) and more than 90% for

malonic to adipic (C_3-C_6) acids. The detection limits of diacids and related compounds were ca. 0.002 ng m^{-3}. The analytical errors in duplicate analyses are within 10% for major species.

To measure water-soluble organic carbon (WSOC), a punch of 20 mm diameter of each QFF was extracted with organic-free ultrapure water in a 50 mL glass vial with a Teflon-lined screw cap under ultrasonication for 15 min. The water extracts were subsequently passed through a syringe filter (Millex-GV, Millipore; diameter of 0.22 μm). The extract was first acidified with 1.2 M HCl and purged with pure air in order to remove dissolve inorganic carbon and then WSOC was measured using a total organic carbon (TOC) analyzer (Shimadzu TOC-V_{CSH}) (Miyazaki et al., 2011). External calibration was performed using potassium hydrogen phthalate before analysis of WSOC. The sample was measured three times and the average value was used for the calculation of WSOC concentrations. The analytical error in the triplicate analysis was 5% with a detection limit of 0.1 μgC m^{-3}.

Organic and elemental carbon (OC and EC) was determined using a Sunset Lab carbon analyzer following the Interagency Monitoring of Protected Visual Environments (IMPROVE) thermal evolution protocol as described by Wang et al. (2005a). A filter disc of 1.5 cm^2 was placed in a quartz tube inside the thermal desorption chamber of the analyzer and then stepwise heating was applied. Helium (He) gas was applied in the first ramp and was switched to mixture of He/O_2 in the second ramp. The evolved CO_2 during the oxidation at each temperature step was measured with non-dispersive infrared (NDIR) detector system. The detection limits of OC and EC were ca. 0.05 and 0.02 μgC m^{-3}, respectively. The analytical errors in the triplicate analysis of the filter sample were estimated to be 5% for OC and EC. EC was detected only in fine fractions. The concentration of total carbon (TC) was calculated by summing the concentrations of OC and EC in each size fraction.

For the determination of major ions, a punch of 20 mm diameter of each filter was extracted with organic-free ultrapure water under ultrasonication. These extracts were filtered through a disc filter (Millex-GV, Millipore; diameter of 0.22 μm) and injected to ion chromatograph (Compact IC 761; Metrohm, Switzerland) for measuring MSA^-, Cl^-, SO_4^{2-}, NO_3^-, Na^+, NH_4^+, K^+, Ca^{2+}, and Mg^{2+} (Boreddy and Kawamura, 2015). Anions were separated on a SI-90 4E Shodex column (Showa

Denko; Tokyo, Japan) using a mixture of 1.8 mM Na_2CO_3 and 1.7 mM $NaHCO_3$ solution at a flow rate of 1.2 mL min^{-1} as an eluent and 40 mM H_2SO_4 for a suppressor. A Metrosep C2-150 Metrohm column was used for cation analysis using a mixture of 4 mM tartaric acid and 1 mM dipicolinic acid solution as an eluent at a flow rate of 1.0 mL min^{-1}. The injected loop volume was 200 μL. The detection limits for anions and cations were ca. 0.1 ng m^{-3}. The analytical error in duplicate analysis was about 10%.

Field blanks were extracted and analyzed like the real samples. However, blank levels were 0.1-5% of real samples. The reported concentrations of organic and inorganic species were corrected for the field blanks. All the chemicals including authentic standards were purchased from Wako Pure Chemical Co. (Japan), except for 14% BF_3/n-butanol (Sigma-Aldrich, USA).

2.3 Backward air mass trajectories and meteorology

The backward trajectories of air masses were computed for the sampling period using the Hybrid Single-Particle Lagrangian Integrated Trajectory (HYSPLIT) model 4.0 developed by the National Oceanic and Atmospheric Administration (NOAA) Air Resources Laboratory (ARL) (Draxler and Rolph, 2013). The seven-day trajectories at 500 m above the ground level for the samples collected in Okinawa are shown in Figure 2. Typical air mass trajectories corresponding to 0900 UTC for the samples collected in Okinawa are shown in Figure S1 in the supporting information.

Meteorological data including ambient temperature, relative humidity and wind speed for each sample period were obtained from Japan Meteorological Agency (http://www/data/jma.go.jp). During our campaign, ambient temperature, relative humidity and wind speed ranged from 11.9 to 26.6 °C (ave. 20.0±2.6 °C), 43.0 to 91.0% (ave. 70.0±12.0%), 0.10 to 10.2 m s^{-1} (ave. 3.73±1.99 m s^{-1}), respectively. The seven-day trajectories along with the meteorological data including precipitation and downward solar radiation flux are shown in Figure S2.

2.4 Estimation of liquid water content (LWC) of aerosol

LWC of aerosol was calculated for the size-segregated samples collected in Okinawa Island using the ISORROPIA II model (Fountoukis and Nenes, 2007). ISORROPIA II is a computationally efficient and rigorous thermodynamic equilibrium model that exhibits robust and rapid convergence

under all aerosol types with high computational speed (Nenes et al., 1998). ISORROPIA II implies the Zdanovskii-Stokes-Robinson equation and treats only the thermodynamics of K^+-Ca^{2+}-Mg^{2+}-NH_4^+-Na^+-SO_4^{2-}-NO_3^--Cl^--H_2O aerosol system to estimate the LWC. Therefore, the measured organic species such as diacids and related compounds are not included in ISORROPIA II. The model was run as "reverse problem", in which temperature, relative humidity and aerosol phase concentrations of water-soluble inorganic ions were used as input for the estimation of aerosol LWC.

3 Results and discussion

3.1 Size-segregated aerosol chemical characteristics

We use 2.1 μm as a split diameter between the fine and coarse mode particles. Table 1 presents the concentrations of inorganic and carbonaceous species in the fine and coarse mode aerosols. Abundances of organic matter (OM) in the atmosphere are generally estimated by multiplying the measured OC mass concentrations with the conversion factor of 1.6 for urban aerosols and 2.1 for aged aerosols (Turpin and Lim, 2001). CHAAMS is located in the outflow region of East Asian aerosols and local anthropogenic activities are insignificant. Because the aerosols reaching to Okinawa are subjected to undergo the atmospheric oxidation during the long-range transport, the fraction of oxygenated organic species is often high (Takami et al., 2007; Irei et al., 2014; Kunwar and Kawamura, 2014). Therefore, we used the conversion factor of 2.1, instead of 1.6 for calculation of OM.

OM was enriched in fine size fractions than the coarse size fractions (Table 1). The elevated level of OM in fine fractions in Okinawa suggests a substantial contribution of organic aerosols primarily from combustion sources and secondarily from photochemical processes during long-range atmospheric transport. The OM in fine mode aerosol in Okinawa may consist of oxygenated organic compounds such as diacids, ω-oxoacids and α-dicarbonyls. Okinawa was strongly affected by long-range transport of continental air masses from Siberia and Mongolia as well as North China and Korea (Figure 2). It is difficult to specify the source regions of air masses for each sample set because the sampling duration was 3-5 days. Each sample contains mixed continental and oceanic air masses. Precipitation may have an insignificant effect on the transport of pollutants from the

source region to Okinawa because air masses were not experienced serious precipitation events during the transport (Figure S2a).

Sulfate is the most abundant anion in fine mode whereas chloride is the dominant anion in coarse mode. The cation budget is largely controlled by ammonium in fine mode whereas sodium is the most abundant cation in coarse mode. The high abundance of SO_4^{2-} in fine particles suggests a significant contribution of anthropogenic sources including industrial emissions in East Asia via long-range transport of aerosols over the western North Pacific Rim. SO_4^{2-} is an anthropogenic tracer of industrial activities whereas NH_4^+ is the secondary product of NH_3 that is largely derived from the agricultural usage of nitrogen-based fertilizers (Pakkanen et al., 2001) and volatilization from soils and livestock waste in East Asia (Huang et al., 2006). The dominant presences of Na^+ and Cl^- in coarse mode suggest a substantial contribution from sea salt. Na^+ and Cl^- are emitted from the ocean surface as relatively larger particles. Substantial amount of NO_3^- was detected in coarse mode, suggesting a formation of $Ca(NO_3)_2$ or $NaNO_3$ in coarse fractions through the reactive adsorption of gaseous HNO_3 onto pre-existing alkaline particles.

The molecular distributions of detected diacids and related compounds in size-segregated aerosols are shown in Figure 3. Table 2 presents the summarized concentrations of those compounds in fine and coarse modes. Oxalic acid (C_2) was found as the most abundant diacid followed by malonic (C_3) and succinic (C_4) acids in all size-segregated aerosols. The predominance of C_2 in size-segregated aerosols is due to the fact that it can be secondarily produced by the photooxidation of anthropogenic and biogenic organic precursors in gas and aqueous-phase (Kawamura and Sakaguchi, 1999; Warneck, 2003; Carlton et al., 2006). C_2 can also be produced primarily from fossil fuel combustion (Kawamura and Kaplan, 1987) and biomass burning (Kundu et al., 2010) in East Asia and long-range transported to Okinawa.

Phthalic (Ph) and adipic (C_6) acids are the next abundant diacids whereas ketomalonic acid (kC_3) is more abundant than C_6 diacid in the size ranges of 0.43-0.65 μm to 0.65-1.1 μm (Figure 3). Ph and C_6 diacids originate from various anthropogenic sources and thus they can be used as anthropogenic tracers. Ph primarily originates from coal burning and vehicular emission whereas photooxidation of aromatic hydrocarbons such as naphthalene and o-xylene derived from

incomplete combustion of fossil fuel form Ph via secondary processes (Kawamura and Kaplan, 1987). Moreover, abundant presence of Ph may also be caused by enhanced emission of phthalates from plastics used in heavily populated and industrialized regions in China and the subsequent long-range atmospheric transport to Okinawa. Phthalic acid esters are used as plasticizers in resins and polymers (Simoneit et al., 2005). They can be released into the air by evaporation because they are not chemically bonded to the polymer. Kawamura and Usukura (1993) reported that C_6 diacid is an oxidation product through the reaction of cyclohexene with ozone (O_3). The high abundances of Ph and C_6 diacids in Okinawa suggest a significant influence of anthropogenic sources in East Asia via long-range transport of aerosols over the western North Pacific Rim.

Azelaic acid (C_9) is more abundant than adjacent suberic (C_8) and decanedioic (C_{10}) acids in all the size-segregated aerosols (Figure 3 and Table 2). Kawamura and Gagosian (1987) proposed that C_9 is a photooxidation product of biogenic unsaturated fatty acids such as oleic acid ($C_{18:1}$) containing a double bond at C-9 position. Unsaturated fatty acids can be emitted from sea surface microlayers and from local vegetation in Okinawa (Kunwar and Kawamura, 2014). Moreover, Okinawa was affected by long-range transport of air masses from Siberia and Mongolia as well as North China and Korea (Figure 2). Such continental air masses can also deliver C_9 via atmospheric processing of unsaturated fatty acids during long-range transport. The abundant presence of C_9 indicates that atmospheric oxidation of unsaturated fatty acids also occurs in Okinawa aerosols during long-range transport. ω-Oxocarboxylic acids and α-dicarbonyls were detected in the Okinawa aerosols. Glyoxylic acid (ωC_2) was identified as the most abundant ω-oxoacid whereas glyoxal (Gly) was more abundant than methylglyoxal (MeGly) in all the sizes. ωC_2 and Gly are the oxidation product of several anthropogenic and biogenic VOCs and primary generated by fossil fuel combustion and biomass burning (Zimmermann and Poppe, 1996; Volkamer et al., 2001), and are further oxidized to C_2 diacid (Myriokefalitakis et al., 2011). The predominance of ωC_2 and Gly indicates their importance as key precursors of C_2 in Okinawa aerosols.

3.2 Inorganic species

The particle size distributions of major ions are shown in Figure 4. Pearson correlation coefficients (r) among the measured ions in different size modes are given in Table 3. Na^+ and Cl^- are mainly derived from the ocean surface as sea salt particles in the marine atmosphere (Kumar et al., 2008; Geng et al., 2009). The size distributions of Na^+ and Cl^- were found to be bimodal with two peaks in coarse mode (Figure 4a and b). Their peaks at 2.1-3.3 or 3.3-4.7 µm and at >11.3 µm suggest that they are of marine origin due to bubble bursting of surface seawater. Andreas (1998) suggested that the sea spray fall into two types that are defined as film and jet bubbles; film bubbles correspond to the size of 0.5-5 µm whereas jet bubbles produce the size of 5-20 µm. Their coarse mode peaks at 2.1-3.3 µm or 3.3-4.7 and >11.3 µm in Okinawa aerosols were associated with film and jet bubbles. We found that size distribution of Mg^{2+} is similar to those of Na^+ and Cl^- with a significant positive correlation to coarse mode Na^+ and Cl^- ($r = 0.98$), suggesting their similar origin and sources.

A high concentration of Ca^{2+} in coarse mode particles demonstrates its contributions from soil dust (Kerminen et al., 1997a; Tsai and Chen, 2006). A lifting of soil dust in continental sites followed by subsequent long-range atmospheric transport to remote marine site is also proposed as an important source of Ca^{2+} (Wang et al., 2005b). Ca^{2+} showed unimodal distribution with a peak at either 2.1-3.3 or 3.3-4.7 µm (Figure 4c). The coarse mode Ca^{2+} is mostly derived from crustal $CaCO_3$, which heterogeneously reacts with acidic gases (HNO_3 and SO_2) (Kerminen et al., 1997a). This formation mechanism is further supported by a strong correlation of coarse mode Ca^{2+} with NO_3^- ($r = 0.98$). There is no correlation between Ca^{2+} and Na^+ or Cl^- ($r = -0.12$ or -0.27), revealing that sea salt contribution of Ca^{2+} is negligible in Okinawa aerosols. This result suggests that long-range transport of soil dust is an important contributor of Ca^{2+} in the marine aerosols from the western North Pacific Rim.

There is natural limestone caves formed by elevated coral reefs in Okinawa Island. Although local limestone dust may also be re-suspended to the atmosphere by wind (Shimada et al., 2015), the local dust contribution to the ambient level of Ca^{2+} in Okinawa may be small. This interpretation can be supported by the fact that Ca^{2+} peaked in lower coarse size range of 2.1-3.3 or 3.3-4.7 µm. It has been suggested that Ca^{2+} is likely associated with upper coarse size range when the contribution of locally produced soil particles is significant (Bian et al., 2014). Smaller coarse

mode Ca^{2+} is likely associated with long-range transported Asian dust to Okinawa. Moreover, concentrations of Ca^{2+} in coarse mode were found to be much higher in OKI-1 (0.51 μg m^{-3}) and OKI-2 (0.60 μg m^{-3}) than that OKI-5 sample (0.15 μg m^{-3}). Backward trajectories also indicated that the air masses originated from Mongolia and Siberia were transported to Okinawa during the collection of OKI-1 and OKI-2 samples whereas OKI-5 sample has an influence of marine air masses. Such air mass origin again indicates a long-range transport of Asian dust from East Asia to the western North Pacific.

Potassium is enriched in biomass burning aerosols and therefore its abundances in fine particles can serve as a diagnostic tracer of biomass burning (Yamasoe et al., 2000). Moreover, contributions of K^+ from sea salt and dust sources are highly variable in regional case studies with its dominance in coarse mode particles. Fresh biomass burning particles mostly reside in the condensation mode at 0.1-0.5 μm in diameter (Kaufman and Fraser, 1997; Kleeman and Cass, 1999). A unimodal size distribution of K^+ was observed in most sample sets (OKI-1 to OKI-4) with a peak at 0.65-1.1 μm in diameter (Figure 4e). The peak of K^+ at 0.65-1.1 μm suggests that biomass burning particles emitted in East Asia might have undergone a growth to a relatively large size by absorbing water vapor from the atmosphere during long-range transport to Okinawa. This interpretation is supported by the fact that K^+ showed a positive correlation with LWC (r = 0.83) in fine mode. The fine mode nss-K^+ accounted for 95% of total K^+ in OKI-2 sample set and 88% of that in OKI-3 sample set when air masses are coming from Siberia and Mongolia as well as North China. The abundant presence of fine mode nss-K^+ in the OKI-2 and OKI-3 samples further indicates a long-range atmospheric transport of biomass burning aerosols from the Asian continent to the western North Pacific Rim.

NO_x is a precursor of NO_3^-, which can be converted to HNO_3 and then react with NH_3 to form NH_4NO_3. A unimodal size distribution of NO_3^- was observed with a peak at 2.1-3.3 or 3.3-4.7 μm in diameter (Figure 4f). It should also be noted that the NO_3^- concentration in coarse mode is much higher than that in fine mode (Table 1). This result suggests that either dust or sea salt particle is the source of coarse mode NO_3^- in Okinawa. Coarse mode NO_3^- is produced by heterogeneous reaction

of gaseous NO_2 or HNO_3 with alkaline metals such as Na^+ and Ca^{2+} as shown in Reactions 1 and 2 (Kouyoumdjian and Saliba, 2006; Seinfeld and Pandis, 2006).

$HNO_{3(g)} + NaCl_{(aq\ and\ s)} \rightarrow NaNO_{3(aq\ and\ s)} + HCl_{(g)}$ …… R-1

$2HNO_{3(g)} + CaCO_{3(s)} \rightarrow Ca(NO_3)_{2(s)} + H_2O + CO_{2(g)}$ …… R-2

As discussed earlier, the air masses originated from Siberia are transported over Mongolia and North China. Asian dust can be transported from the Asian continent to Okinawa. Therefore, it is possible that the gaseous HNO_3 might already have reacted with $CaCO_3$ (mineral dust particle) to from NO_3^- before arriving to Okinawa through R-2. We found that coarse mode Na^+, which is derived from sea salts, is negatively correlated (r = -0.30) with coarse mode NO_3^-. Although this correlation is not significant (p = 0.51), the negative correlation may indicate some reactive loss of NO_3^- from sea salt particles in coarse mode in Okinawa. NO_3^- peaked at the same particle size of Ca^{2+}. Therefore, NO_3^- in Okinawa coarse mode aerosols was probably resulted from the uptake of HNO_3 gas by soil dust particles enriched with Ca^{2+} via heterogeneous reaction near the source regions. This process is further supported by a good correlation between NO_3^- and Ca^{2+} (r = 0.98) in coarse mode.

The particle size distributions of SO_4^{2-}, which is a major source of acid deposition (Pakkanen et al., 2001), have been the subject of numerous studies in the past few decades (Huang et al., 2006; Kouyoumdjian and Saliba, 2006). Condensation mode SO_4^{2-} arises from gas-phase oxidation of SO_2 followed by gas-to-particle conversion whereas fine mode SO_4^{2-} is formed through aqueous-phase oxidation of SO_2 in aerosols and cloud droplets (Seinfeld and Pandis, 1998). SO_4^{2-} on coarse mode can be attributed to a combination of sulfate and heterogeneous reactions of SO_2 on soil dust or sea salt particles (Seinfeld and Pandis, 1998; Pakkanen et al., 2001). A unimodal size distribution of SO_4^{2-} was observed with a peak at 0.65-1.1 μm (Figure 4g). Gao et al. (2012) suggested that in-cloud process produces SO_4^{2-} as larger particles by aqueous-phase oxidation of SO_2 in cloud droplets. Therefore, the peak of SO_4^{2-} at 0.65-1.1 μm in Okinawa may be involved with aqueous-phase oxidation of SO_2 in aerosols.

Size distribution of methanesulfonate (MSA^-) is similar to that of SO_4^{2-} (Figure 4i) in Okinawa. MSA^- showed a strong correlation with SO_4^{2-} (r = 0.89) in fine mode, suggesting that MSA^- should

have similar origin with SO_4^{2-} in fine mode. Although MSA^- is produced by gas-to-particle conversion via the oxidation of dimethyl sulfide (DMS) emitted from the ocean (Quinn et al., 1993; Kerminen et al., 1997b), there is some indirect evidence that liquid-phase production might also be possible (Jefferson et al., 1998). Biomass burning also produces DMS in the atmosphere (Meinardi et al., 2003; Geng and Mu, 2006). MSA^- showed high correlation with K^+ or NH_4^+ (r = 0.92) in fine mode, indicating that an enhanced emission of DMS from biomass burning followed by the subsequent oxidation during long-range transport may have contributed significantly to fine mode MSA^- in Okinawa. Moreover, MSA^- can also be produced in fine mode by the oxidation of DMS that is emitted from marine phytoplankton in the surrounding ocean. It is noteworthy that East Asian aerosols travelled over the marine regions including the East China Sea, Sea of Japan and Pacific Ocean during long-range atmospheric transport. The size distribution of MSA^- observed over Okinawa is consistent with previous studies from the China Sea by Gao et al. (1996), who suggested that MSA is produced through the oxidation of S-containing species in the marine atmosphere.

NH_4^+ in the Okinawa aerosols shows a unimodal size distribution with a peak at 0.65-1.1 μm (Figure 4h), indicating that NH_4^+ is mainly formed by gas-to-particle conversion via the reaction with H_2SO_4 and HNO_3. Interestingly, the size distribution of NH_4^+ is similar to that of SO_4^{2-} and diacids such as oxalic acid (Figure 4g and 5a). We also found a strong correlation between SO_4^{2-} and NH_4^+ on fine mode (r = 0.99). Ion balance calculations are commonly used to evaluate acid-base balance of aerosol particles. Average equivalent ratios of total cations (Na^+, NH_4^+, K^+, Mg^{2+} and Ca^{2+}) to anions (Cl^-, NO_3^- and SO_4^{2-}) in fine fractions varied from 0.75 for the size bin of 0.65-1.1 μm to 0.86 for the size bin of 1.1-2.1 μm, indicating that fine mode aerosols in Okinawa were apparently acidic.

NH_3 is an alkaline gas that neutralizes the acidic particles in the atmosphere. Kerminen et al. (1997a) proposed that particulate NH_4^+ is secondarily formed via heterogeneous reactions of gaseous NH_3 with acidic species (H_2SO_4 and HNO_3). The reaction of NH_3 with H_2SO_4 is favored over its reaction with HNO_3. The average NH_4^+/SO_4^{2-} equivalent ratios in fine mode particles in Okinawa varied from 0.36 for the size bin of 1.1-2.1 μm to 0.81 for the size bin of 0.43-0.65 μm,

indicating that NH_3 was not abundant enough to neutralize all SO_2. The aerosol chemical composition data obtained from the ISORROPIA II model revealed that significant amounts of SO_4^{2-}, HSO_4^- and NH_4^+ in fine mode were present in liquid-phase whereas SO_4^{2-} and NO_3^- were mainly present as solid-phase in the coarse mode aerosols in the forms of $CaSO_4$ and $Ca(NO_3)_2$, respectively. Interestingly, the average NH_4^+/SO_4^{2-} equivalent ratios in coarse mode particles ranged from 0.01 for the size bin >11.3 μm to 0.09 for the size bins of 2.1-3.3 and 3.3-4.7 μm, suggesting that coarse mode aerosols in Okinawa were also NH_4^+-poor. This result further indicates that there was not enough NH_3 to neutralize HNO_3, and thus shortfall of NH_3 may be the restrictive factor for the formation of NH_4NO_3 in Okinawa aerosols. Therefore, NO_3^- reacts with coarse particles that contain alkaline species (Ca^{2+}) in Okinawa aerosols.

The size distribution of SO_4^{2-} depends on the concentration of NH_4^+, richness of NH_3 in the air, and the presence of coarse mode particles. SO_4^{2-} and NH_4^+ often coexist in fine mode because H_2SO_4 condenses on this mode as fine particles that have more surface area (Jacobson, 2002). Although NH_3 was not abundant enough to neutralize all SO_4^{2-}, most of SO_4^{2-} might be neutralize by NH_3 in fine mode. Hence, SO_4^{2-} is enriched in fine mode rather than being associated with dust particles. An enrichment of NO_3^- in the dust fraction in our study is supported by the laboratory studies of Hanisch and Crowley (2001a, 2001b), who found a large and irreversible uptake between HNO_3 and various authentic dust samples including samples from Chinese dust region.

3.3 Water-soluble organic carbon (WSOC) and organic carbon (OC)

The mass-based size distribution of WSOC is characterized by a major peak at 0.65-1.1 μm in fine mode and by a small peak at 3.3-4.7 μm in coarse mode (Figure 6a and Table 1). Huang et al. (2006) observed that fine mode WSOC was primarily derived from combustion sources and secondarily produced in the atmosphere by the photochemical oxidation of VOCs. The WSOC concentrations showed a strong correlation with fine mode SO_4^{2-} (r = 0.96). Because production of SO_4^{2-} is closely linked to photochemical activity, this result suggests an important secondary production of WSOC in fine mode particles during long-range atmospheric transport from East Asia. WSOC concentrations also showed high correlation with K^+ (r = 0.93) and NH_4^+ (r = 0.91) in fine mode. This result suggests that direct emission from biomass burning or fast oxidation of

biomass burning-derived precursors significantly contributes to the formation of fine mode WSOC in Okinawa aerosols during long-range transport.

The mass-size distribution pattern of OC is similar to that of WSOC with a major peak in the size range of 0.65-1.1 μm whereas a small peak was appeared in the size range of 3.3-4.7 μm in diameter (Figure 6b). Primary emission from biomass burning and/or photooxidation of biomass burning derived precursors might be a dominant source of fine mode OC in Okinawa aerosols. This interpretation is supported by the fact that OC showed a strong correlation (r = 0.95) with K^+ in fine mode. The fine mode OC showed significant positive correlations with SO_4^{2-} (r = 0.93) and NH_4^+ (0.91), suggesting a secondary photochemical formation of OC in fine mode of Okinawa aerosols.

A significant portion of OC may be oxidized to WSOC during the atmospheric transport from East Asia to the western North Pacific. The mass ratio of WSOC/OC has been proposed as a measure of photochemical processing or aging of organic aerosols especially in long-range transported aerosols (Aggarwal and Kawamura, 2009). The WSOC/OC ratios varied from 0.51-0.76 with an average of 0.67±0.09 in the fine mode and 0.43-0.63 with an average of 0.55±0.09 in the coarse mode. The higher WSOC/OC ratio in fine mode suggests that organics are significantly subjected to photochemical processing in fine aerosols during long-range transport from the Asian continent to Okinawa than coarse mode aerosols.

Source contributions and secondary processes that may convert VOCs to amore soluble forms on the surface area of fine particles could cause higher WSOC/OC ratios in fine mode. Biomass burning-derived OC is highly water-soluble and usually resides in fine mode whereas coarse mode OC contains high molecular weight organic compounds emitted by soil resuspension and emissions of pollens and fungal spores, which are less water-soluble (Wang et al., 2011; Mkoma et al., 2013). Biomass burning significantly contributed to fine mode WSOC in Okinawa as discussed above. Moreover, accumulation of gas-phase precursors of WSOC may occur preferentially in the particle size with the greatest surface area (Kanakidou et al., 2005). It has been proposed that fine particles offer more surface area and thus reaction rate is more on the surface of fine particles than coarse particles (Kanakidou et al., 2005). The higher WSOC/OC ratio in fine particles than coarse particles

has also been observed in long-range transported East Asian aerosols over Northern Japan (Agarwal et al., 2010).

The WSOC/OC ratio in fine mode showed a weak positive correlation with downward solar radiation flux (r = 0.39). This weak correlation is probably due to the fact that fine mode WSOC can be produced in aqueous-phase of aerosols during long-range transport. Based on the year round measurements of TSP aerosols from Okinawa Island, Kunwar and Kawamura (2014) documented higher WSOC/OC ratio in winter (ave. 0.60) and spring (ave. 0.45) than summer (ave. 0.28). These observations demonstrate that WSOC can be produced from OC under weak solar radiation condition on the transport pathway from the source region to Okinawa possibly via aqueous-phase processing.

Calculated LWC for each sample from Okinawa and average LWC in size-segregated aerosols are shown in Figure 7. The highest LWC was found at the size of 0.65-1.1 μm in the fine mode in Okinawa samples. WSOC can also contribute to aerosol LWC although their ability to absorb water is significantly less than that of inorganics (Ansari and Pandis, 2000; Speer et al., 2003; Engelhart et al., 2011). Moreover, organic species are not taken into account in ISORROPIA II for the calculation of LWC. It is noteworthy that WSOC/OC ratio and LWC in fine mode significantly correlate with r = 0.87 whereas negative correlation was found in coarse mode (r = -0.19), suggesting a possible production of WSOC from OC in aerosol aqueous-phase in fine mode of Okinawa aerosols. There may also be another important sources of fine mode WSOC in Okinawa aerosols such as primary emission from biomass burning and secondary formation via gas-phase photochemical reactions during long-range atmospheric transport (Hagler et al., 2007; Lim et al., 2010). This result may indicate that shorter-chain diacids and related polar compounds can contribute more to fine mode WSOC via oxidation of various organic precursors during long-range transport (Carlton et al., 2007; Kawamura et al., 2005, 2007; Miyazaki et al., 2010).

3.4 Dicarboxylic acids and related compounds

The size distributions of selected diacids and related compounds are shown in Figure 5. Based on the sources and formation processes, their size distributions fall into two groups: a group with a dominant fine mode and a group with a dominant coarse mode as discussed in the ensuing sections.

443 **3.4.1 C_2, ωC_2, Gly, Ph and benzoic acid**

444 The first group, including C_2, ωC_2, Gly, Ph and benzoic acid, showed the similar size distributions
445 with maxima in fine mode. C_2 showed a peak at 0.65-1.1 μm in fine mode (Figure 5a). The size
446 distribution of C_2 in Okinawa is different from that observed off the coast of East Asia by Mochida
447 et al. (2003a, 2007), who found a strong bimodal pattern of C_2 with a peak in the coarse mode. They
448 suggested that the coarse mode peak of C_2 was emerged by the uptake of gaseous diacids or
449 heterogeneous oxidations of organic precursors on the dust and sea salt particles during long-range
450 transport. The unimodal distribution of C_2 in Okinawa with maxima in fine mode suggests that the
451 heterogeneous uptake of C_2 on dust and sea-salt particles did not occur.

452 The condensation mode of C_2 is likely produced photochemically in the gas-phase followed by
453 condensation onto pre-existing particles at 0.1-0.5 μm (Huang et al., 2006). The fine mode peak of
454 C_2 at the size of 0.65-1.1 μm in Okinawa aerosols suggests a preferential production of C_2 via the
455 oxidation of precursors in aerosol aqueous-phase during long-range atmospheric transport. We
456 found that size distribution of C_2 diacid is similar to that of SO_4^{2-} (Figure 4g and 5a), suggesting a
457 secondary formation of C_2 possibly in aerosol aqueous-phase. The good correlations of C_2 with
458 SO_4^{2-} (r = 0.92) and NH_4^+ (0.89) in fine mode further supports that C_2 is a secondary photochemical
459 product. Fine mode C_2 can also be produced primarily from fossil fuel combustion and biomass
460 burning in East Asia and long-range transported to Okinawa. C_2 diacid showed a significant
461 positive correlation with fine mode K^+ (r = 0.85), indicating that biomass burning contributed
462 significantly to fine mode C_2 in Okinawa aerosols.

463 Lim et al. (2005) and Legrand et al. (2007) reported the formation of diacids in aqueous-phase.
464 Here we investigate the impact of LWC on the formation of diacids in Okinawa aerosols. LWC of a
465 particle can influence the production of C_2 via the changes in gas/particle partitioning of organic
466 precursors and subsequent heterogeneous reaction in aerosol aqueous-phase. A strong positive
467 correlation (r = 0.92) of C_2 with LWC was found in fine mode whereas the correlation was negative
468 in coarse mode (r = -0.29), indicating a possible aqueous-phase production of C_2 via the oxidation
469 of C_2 precursors in fine mode. Several secondary formation pathways are known to C_2 in
470 atmospheric aerosols. C_2 is produced by the decay of its higher homologues (C_3-C_5 diacids) or

oxidation of unsaturated fatty acids such as oleic acid ($C_{18:1}$) followed by the degradation to shorter-chain diacids in aqueous-phase (Kawamura and Ikushima, 1993; Kawamura and Sakaguchi, 1999; Pavuluri et al., 2015). C_2 can also be produced by the aqueous-phase oxidation of ωC_2, which can be formed by aqueous oxidation of Gly and MeGly produced by the oxidation of various VOCs including toluene, ethene and isoprene (Zimmermann and Poppe, 1996; Volkamer et al., 2001; Lim et al., 2005; Carlton et al., 2006; Ervens et al., 2008).

The scatter plots of C_2 with C_3-C_5 diacids in fine and coarse modes are shown in Figure S3. The robust correlations of C_2 with C_3-C_5 diacids (r = 0.89-0.92) were found in fine mode, indicating that they might have similar sources and origin or C_2 may be produced via the decay of its higher homologues (C_3-C_5 diacids) during long-range transport. The differences in the slopes of linear regression of C_2 with C_3 and C_4 diacids between fine and coarse modes are not significant but slopes are slightly higher in fine mode than the coarse mode (Figure S3a-d and Table S1). Interestingly, significantly higher slope was observed for regression line between C_2 and glutaric (C_5) acid in fine mode than coarse mode (Figure S3e-f and Table S1). It is also noteworthy that the slope of regression line of C_2 with C_5 diacid is significantly higher than that for C_3 and C_4 diacids in fine mode (Figure S3a, c, e and Table S2). These results indicate that fine mode oxalic acid may be produced from oxidation of glutaric acid during long-range transport via succinic and malonic acids as intermediates. The laboratory studies of Hatakeyama et al. (1985) and Kalberer et al. (2010) have documented that glutaric acid is produced by the oxidation of cyclohexene by O_3, which can be further oxidized in aqueous-phase to result in oxalic acid (Kawamura and Sakaguchi, 1999; Legrand et al., 2007). This interpretation is further supported by the fact that C_3-C_5 diacids were enriched in the fine mode of most samples (Figure 5b-d) and showed good correlations with LWC (r = 0.82-0.89) possibly due to the enhanced secondary production by the oxidation of its precursor compounds in aerosol aqueous-phase.

The size distribution of ωC_2 and Gly is similar to that of C_2 diacid in the Okinawa samples (Figure 5e and f). The enrichment of ωC_2 and Gly in fine mode may be associated with enhanced secondary formation via aqueous-phase processing of their precursors during long-range transport. This interpretation is evidenced by the fact that strong correlations of ωC_2 and Gly were found with

499 SO_4^{2-} (r = 0.96 and 0.86, respectively) and LWC (0.95) in fine mode. The fine mode ωC_2 and Gly
500 can also be produced primarily from biomass burning in East Asia and long-range transported to
501 Okinawa. Significant positive correlations between ωC_2 and K^+ (r = 0.90), and Gly and K^+ (0.86)
502 suggest that biomass burning contributed significantly to the fine mode ωC_2 and Gly in Okinawa
503 aerosols. Gly is a well-known precursor of ωC_2 and C_2 in atmospheric aerosols (Lim et al., 2005;
504 Ervens et al., 2010; Myriokefalitakis et al., 2011). The preferential enrichment of Gly and ωC_2 in
505 fine mode can form C_2 in Okinawa aerosols by aqueous-phase processing.

506 High correlations among C_2, ωC_2 and Gly in fine mode (r = 0.92-0.99) also indicate their similar
507 sources and formation processes and that C_2 diacid may be produced by the oxidation of ωC_2 and
508 Gly in fine mode. There is no significant difference in the slope of regression line of C_2 with ωC_2
509 between the fine and coarse modes (Figure S3g-h and Table S1) whereas the slope of regression
510 line of C_2 with Gly is significantly higher in fine mode than coarse mode (Figure S3i-j and Table
511 S1). It is also remarkable that the slope of linear regression of C_2 with Gly is significantly higher
512 than that with ωC_2 in fine mode (Figure S3g-i and Table S2). This result may indicate a possible
513 formation of fine mode oxalic acid from glyoxal via glyoxylic acid as an intermediate during long-
514 range atmospheric transport in the western North Pacific.

515 The enrichment of C_2, ωC_2 and Gly in fine mode in Okinawa was probably due to the enhanced
516 oxidation of anthropogenic precursors emitted in East Asia during long-range transport because
517 their size distributions are consistent with that of Ph and benzoic acid (Figure 5g and h), which are
518 tracers of anthropogenic sources. The strong correlations of fine mode C_2, ωC_2 and Gly with Ph (r =
519 0.85-0.93) and benzoic acid (r = 0.90-0.96) further suggest that anthropogenic precursors are their
520 important sources in fine mode. Ph and benzoic acid are directly emitted from combustion sources
521 and secondarily produced in the atmosphere by the photooxidation of aromatic hydrocarbons
522 emitted from the incomplete combustion of fossil fuel (Kawamura et al., 1985; Kawamura and
523 Kaplan, 1987; Ho et al., 2006).

524 Aromatic hydrocarbons such as naphthalene and toluene have been suggested as major
525 precursors of Ph and benzoic acid, respectively (Schauer et al., 1996; Kawamura and Yasui, 2005).
526 Based on the high levels of naphthalene and toluene in China (Liu et al., 2007; Tao et al., 2007;

Duan et al., 2008), Ho et al. (2015) recently suggested that oxidation of naphthalene and toluene in the atmosphere is one of major source of Ph and benzoic acid, respectively. High levels of precursors in the source regions might favor the significant secondary production of Ph and benzoic acid during long-range transport in the western North Pacific. It may be possible that their precursors emitted in East Asia were taken up by aqueous-phase aerosol and oxidized to result in Ph and benzoic acid in fine mode during long-range transport. Moreover, enrichment of Ph and benzoic acid in fine mode further suggests that these species are associated with combustion sources either by primary emission and/or secondary production from the precursor compounds, being consistent with other anthropogenic SO_4^{2-}, NH_4^+ and K^+. Fine mode Ph can also be produced from evaporation of phthalates from plastics used in populated and industrialized regions in East Asia and long-range transported to Okinawa as discussed earlier. This explanation is consistent with the enrichment of terephthalic acid (tPh) in fine mode (Figure 5i), which is a tracer of plastic burning (Kawamura and Pavuluri, 2011).

3.4.2 C_9 and ωC_9

The second group of organic compounds, including C_9 and ωC_9, showed bimodal size distribution with a major peak on coarse mode at 3.3-4.7 μm and minor peak on fine mode at 0.65-1.1 μm (Figure 5j and k). The strong correlations were found between C_9 and Na^+ (r = 0.85), and ωC_9 and Na^+ (0.83) in coarse mode, indicating that C_9 and ωC_9 may be emitted into the atmosphere from the sea surface microlayers together with sea salt particles in Okinawa. Kawamura and Gagosian (1987) suggested that C_9 and ωC_9 are also derived from the photooxidation of unsaturated fatty acids such as oleic acid ($C_{18:1}$) that are produced by phytoplankton and emitted from sea surface microlayers as sea salt particles. The laboratory experiments also documented the formation of C_9 and ωC_9 due to photooxidation of $C_{18:1}$ (Matsunaga et al., 1999; Huang et al., 2005; Ziemann, 2005; Tedetti et al., 2007). Sea surface microlayers in the surroundings of Okinawa can also emit unsaturated fatty acids together with sea salts. Therefore, the major peaks of C_9 and ωC_9 on the coarse mode may be derived from heterogeneous oxidation of unsaturated fatty acids of marine phytoplankton origin on the sea salt particles.

554 Wang et al. (2011) suggested that unsaturated fatty acids can be directly emitted as fine particles
555 from food cooking emission in urban area in China and be oxidized to C_9 diacid in fine mode. The
556 minor peak of C_9 and ωC_9 in fine mode can be explained by the oxidation of fine-mode unsaturated
557 fatty acids derived from food cooking or gaseous unsaturated fatty acids during long-range transport
558 to the western North Pacific.

559 **3.5 Ratios of selected diacids**

560 Kawamura and Ikushima (1993) proposed that malonic to succinic acid ratio (C_3/C_4) is a tracer to
561 evaluate the extent of photochemical processing of organic aerosols. Because C_4 is oxidized to C_3,
562 an increase in the C_3/C_4 ratio indicates an increased photochemical processing. The average C_3/C_4
563 ratio in sum of all the size fractions was found to be 1.5±0.1 in Okinawa aerosols. This result
564 suggests that the extent of photochemical processing is much greater in Okinawa than Los Angeles
565 (0.35) (Kawamura and Kaplan, 1987) but similar to that of urban Tokyo (1.5) (Kawamura and
566 Ikushima, 1993), whereas it is lower than those of marine aerosols at Chichijima Island in the
567 western North Pacific (2.0) (Mochida et al., 2003b) and the remote Pacific including tropics (3.9)
568 (Kawamura and Sakaguchi, 1999). Figure 8a shows changes in the C_3/C_4 ratios as a function of
569 particle size. The C_3/C_4 ratios exhibit higher values at 1.1-2.1 μm in fine mode and at 2.1-3.3 and
570 3.3-4.7 μm in coarse mode. This result suggests that C_3 production via C_4 decomposition occurs
571 more efficiently at these size ranges by aqueous-phase processing.

572 Ph diacid originates from various anthropogenic sources whereas C_9 diacid is specifically
573 produced by the oxidation of biogenic unsaturated fatty acids (Kawamura and Gagosian, 1987;
574 Kawamura and Ikushima, 1993). Therefore, Ph/C_9 ratio is most likely used as a tracer to understand
575 the source strength of anthropogenic v.s. biogenic sources of diacids. Higher Ph/C_9 ratio shows
576 more influence of anthropogenic sources whereas lower ratio shows more influence of biogenic
577 sources. Figure 8b presents changes in the ratios of Ph/C_9 as a function of particle sizes. The higher
578 Ph/C_9 ratios were obtained on fine mode particles than coarse mode particles. These results suggest
579 that fine aerosols in Okinawa are significantly influenced by anthropogenic sources whereas the
580 coarse aerosols are more influenced by biogenic sources. A significant contribution of Ph on fine

581 mode further supports that anthropogenic sources are an important source of diacids and related
582 compounds in fine mode of Okinawa aerosols.

583 **4 Summary and conclusions**

584 Nine-stage atmospheric particles from <0.43 to >11.3 μm in diameter, collected in spring 2008 at
585 Cape Hedo, Okinawa in the western North Pacific Rim, were analyzed for water-soluble diacids
586 and related compounds as well as water-soluble organic carbon (WSOC), organic carbon (OC) and
587 inorganic ions. The molecular distributions of diacids were characterized by the predominance of
588 oxalic acid (C_2) followed by malonic (C_3) and succinic (C_4) acids in all stages, suggesting that they
589 are most likely produced by the photooxidation of VOCs and particulate organic precursors in the
590 source region and/or during long-range atmospheric transport. The abundant presence of SO_4^{2-} as
591 well as phthalic and adipic acids in Cape Hedo suggested a significant contribution of
592 anthropogenic sources including industrial emissions in East Asia to Okinawa aerosols via long-
593 range atmospheric transport.

594 SO_4^{2-}, NH_4^+, and diacids up to 5-carbon atoms as well as glyoxylic acid (ωC_2) and glyoxal (Gly)
595 showed good correlations with peaks in fine mode (0.65-1.1 μm). WSOC and OC also peaked on
596 fine mode with an additional minor peak on coarse mode. Similar size distributions and strong
597 correlations of diacids (C_2-C_5), ωC_2 and Gly with SO_4^{2-} in fine mode suggest their secondary
598 formation possibly in aerosol aqueous-phase. Their strong correlations with LWC in fine mode
599 further suggest an importance of the aqueous-phase production in Okinawa aerosols. They may
600 have also been directly emitted from biomass burning as supported by strong correlations with K^+
601 in fine mode. The robust correlations of C_2 with C_3-C_5 diacids as well as ωC_2 and Gly indicate that
602 they are the key precursors of C_2 diacid in Okinawa aerosols.

603 Longer-chain diacid (C_9) and ω-oxoacid (ωC_9) showed bimodal size distribution with a major
604 peak on coarse mode, suggesting that they were directly emitted and/or produced by photooxidation
605 of unsaturated fatty acids mainly derived from sea surface microlayers via heterogeneous reactions
606 on sea spray particles. We observed that WSOC and OC in fine particles are photochemically more
607 processed in the atmosphere than in coarse particles during long-range transport. This study

608 demonstrates that anthropogenic and biomass burning aerosols emitted from East Asia have
609 significant influence on the molecular compositions of water-soluble organic aerosols in the
610 western North Pacific Rim.

611 **Acknowledgement**

612 We acknowledge the financial support from the Japan Society for the Promotion of Science (JSPS)
613 through Grant-in-Aid Nos. 1920405 and 24221001. We appreciate the financial support of the JSPS
614 fellowship to D. K. Deshmukh. We also acknowledge the support of ENSCR to M. Lazaar for the
615 summer student program in Japan. The authors gratefully appreciate the NOAA Air Resources
616 Laboratory (ARL) for the provision of the HYSPLIT transport and dispersion model
617 (http://www.ready.noaa.gov) for seven-day air mass backward trajectories of sampling site Cape
618 Hedo for each sampling period. We thank E. Tachibana for the analyses of OKI-5 samples and M.
619 Mochida, S. Aggarwal and Y. Kitamori for the helps during the campaign. The authors appreciate
620 the critical and useful comments by anonymous reviewers, which significantly improved the quality
621 of manuscript.

622

References

Ansari, A. S. and Pandis, S. N.: Water absorption by secondary organic aerosol and its effect on inorganic aerosol behavior, Environ. Sci. Technol., 34, 71-77, 2000.

Agarwal, S., Aggarwal, S. G., Okuzawa, K., and Kawamura, K.: Size distributions of dicarboxylic acids, ketoacids, alpha-dicarbonyls, sugars, WSOC, OC, EC and inorganic ions in atmospheric particles over Northern Japan: implication for long-range transport of Siberian biomass burning and East Asian polluted aerosols, Atmos. Chem. Phys., 10, 5839-5858, 2010.

Aggarwal, S. G. and Kawamura, K.: Carbonaceous and inorganic composition in long-range transported aerosols over northern Japan: implicationsn for aging of water-soluble organic fraction, Atmos. Environ., 43, 2532-2540, 2009.

Andreas, E.L.: A new sea spray generation function for wind speeds up to 32 m s^{-1}, J. Phys. Oceanogr., 28, 2175-2184, 1998.

Bian, Q., Huang, X. H. H., and Yu, J. Z.: One-year observations of size distribution characteristics of major aerosol constituents at a costal site in Hong Kong - Part 1: Inorganic ions and oxalate, Atmos. Chem. Phys., 14, 9013-9027, 2014.

Boreddy, S. K. R. and Kawamura K.: A 12-year observation of water-soluble inorganic ions in TSP aerosols collected at a remote marine location in the western North Pacific: An outflow region of Asian dust, Atmos. Chem. Phys., 15, 6437-6453, 2015.

Carlton, A. G., Turpin, B. J., Altieri, K. E., Seitzinger, S., Reff, A., Lim, H. J., and Ervens, B.: Atmospheric oxalic acid and SOA production from glyoxal: Results of aqueous photooxidation experiments, Atmos. Environ., 41, 7588-7602, 2007.

Carlton, A. G., Turpin, B. J., Lim, H. J., Altieri, K. E., and Seitzinger, S.: Link between isoprene and secondary organic aerosol (SOA): Pyruvic acid oxidation yields low volatility organic acids in clouds, Geophys. Res. Lett., 33, L06822, doi:10.1029/2005GL025374, 2006.

Davidson, C. I., Phalen, R. F., and Solomon, P. A.: Airborne particulate matter and human health: A review, Aerosol. Sci. Tech., 39, 737-749, 2005.

Draxler, R. R. and Rolph, G. D.: HYSPLIT (HYbrid Single-Particle Lagrangian Integrated Trajectory) Model, available at: http://www.arl.noaa.gov/HYSPLIT.php (last access: 5 January 2015), NOAA Air Resouces Laboratory, College Park, MD.

Duan, J. C., Tan, J. H., Yang, L., Wu, S., and Hao, J. M.: Concentration, sources and ozone formation potential of volatile organic compounds (VOCs) during ozone episode in Beijing, Atmos. Res., 88, 25-35, 2008.

Engelhart, G. J., Hildebrandt, L., Kostenidou, E., Mihalopoulos, N., Donahue, N. M., and Pandis, S. N.: Water content of aged aerosol, Atmos. Chem. Phys., 11, 911-920, 2011.

Engling, G., Lee, J. J., Sie, H. J., Wu, Y. C., and Yet-Pole, I.: Anhydrosugar characteristics in biomass smoke aerosol-case study of environmental influence on particle-size of rice straw burning aerosol, J. Aerosol Sci., 56, 2-14, 2013.

Irei, S., Takami, A., Hayashi, M., Sadanaga, Y., Hara, K., Kaneyasu, N., Sato, K., Arakaki, T., Hatakeyama, S., Bandow, H., Hikida, T., and Shimono, A.: Transboundary secondary organic

aerosol in western Japan indicated by the $\delta^{13}C$ of water-soluble organic carbon and the *m*/*z* 44 signal in organic aerosol mass spectra, Environ. Sci. Technol., 48, 6273-6281, 2014.

Ervens, B., Carlton, A. G., Turpin, B. J., Altieri, K. E., Kreidenweis, S. M., and Feingold, G.: Secondary organic aerosol yields from cloud-processing of isoprene oxidation products, Geophys. Res. Lett., 35, L02816, doi:10.1029/2007gl031828, 2008.

Ervens, B., Cubison, M., Andrews, E., Feingold, G., Ogren, J. A., Jimenez, J. L., DeCarlo, P., and Nenes, A.: Prediction of cloud condensation nucleus number concentration using measurements of aerosol size distributions and composition and light scattering enhancement due to humidity, J. Geophys. Res., 112, D10S32, doi:10.1029/2006jd007426, 2007.

Ervens, B. and Volkamer, R.: Glyoxal processing by aerosol multiphase chemistry: towards a kinetic modeling framework of secondary organic aerosol formation in aqueous particles, Atmos. Chem. Phys., 10, 8219-8244, 2010.

Falkovich, A. H., Graber, E. R., Schkolnik, G., Rudich, Y., Maenhaut, W., and Artaxo, P.: Low molecular weight organic acids in aerosol particles from Rondonia, Brazil, during the biomass-burning, transition and wet periods, Atmos. Chem. Phys., 5, 781-797, 2005.

Fountoukis, C. and Nenes, A.: ISORROPIA II: a computationally efficient thermodynamic equilibrium model for K^+-Ca^{2+}-Mg^{2+}-NH_4^+-Na^+-SO_4^{2-}-NO_3^--Cl^--H_2O aerosols, Atmos. Chem. Phys., 7, 4639-4659, 2007.

Gao, Y., Arimoto, R., Duce, R. A., Chen, L. Q., Zhou, M. Y., and Gu, D. Y.: Atmospheric non-sea-salt sulfate, nitrate and methanesulfonate over the China Sea, J. Geophys. Res., 101, 12601-12611, 1996.

Gao, X., Xue, L., Wang, X., Wang, T., Yuan, T., Gao, R., Zhou, Y., Nie, W., Zhang, Q., and Wang, W.: Aerosol ionic components at Mt. Heng in central southern China: abundances, size distribution, and impacts of long-range transport, Sci. Total Environ., 433, 498-506, 2012.

Geng, H., Park, Y., Hwang, H., Kang, S., and Ro, C. U.: Elevated nitrogen-containing particles observed in Asian dust aerosol samples collected at the marine boundary layer of the Bohai Sea and the Yellow Sea, Atmos. Chem. Phys., 9, 6933-6947, 2009.

Geng, C. and Mu, Y: Carbonyl sulfide and dimethyl sulfide exchange between trees and the atmosphere, Atmos. Environ., 40, 1373-1383, 2006.

Hagler, G. S. W., Bergin, M. H., Smith, E. A., and Dibb, J. E.: A summer time series of particulate carbon in the air and snow at Summit, Greenland, J. Geophys. Res., 112, D21309, doi:10.1029/2007JD008993, 2007.

Hanisch, F. and Crowley, J.N.: Heterogeneous reactivity of gaseous nitric acid on Al_2O_3, $CaCO_3$, and atmospheric dust samples: A Knudsen cell study, J. Phys.Chem. (A), 105, 3096-3106, 2001a.

Hanisch, F. and Crowley, J.N.: The heterogeneous reactivity of gaseous nitric acid on authentic mineral dust samples, and on individual mineral and clay mineral components, Phys. Chem. Chem. Phys., 3, 2474-2482, 2001b.

Hatakeyama, S., Tanonaka, T., Weng, J., Bandow, H., Takagi, H., and Akimoto, H.: Ozone-cyclohexene reaction in air: quantitative analyses of particulate products and the reaction mechanism, Environ. Sci. Technol., 19, 935-942, 1985.

Ho, K. F., Lee, S. C., Cao, J. J., Kawamura, K., Watanabe, T., Cheng, Y., and Chow, J. C.: Dicarboxylic acids, ketocarboxylic acids and dicarbonyls in the urban roadside area of Hong Kong, Atmos. Environ., 40, 3030-3040, 2006.

Ho, K. F., Huang, R. -J., Kawamura, K., Tachibana, E., Lee, S. C., Ho, S. S. H., Zhu, T., and Tian, L.: Dicarboxylic acids, ketocarboxylic acids, α-dicarbonyls, fatty acids and benzoic acid in $PM_{2.5}$ aerosol collected during CAREBeijing-2007: an effect of traffic restriction on air quality, Atmos. Chem. Phys., 15, 3111-3123, 2015.

Huang, H. -M., Katrib, Y., and Martin, S. C.: Products and mechanisms of the reaction of oleic acid with ozone and nitrate radical, J. Phys. Chem. A, 109, 4517-4530, 2005.

Huang, X. F., Yu, J. Z., He, L. Y., and Yuan, Z. B.: Water-soluble organic carbon and oxalate in aerosols at a coastal urban site in China: Size distribution characteristics, sources, and formation mechanisms, J. Geophys. Res., 111, D22212, doi:10.1029/2006JD007408, 2006.

Jacobson, M. Z.: Atmospheric Pollution: History, Science, and Regulation. Cambridge University Press, United Kingdom, 2002.

Jacobson, M. C., Hansson, H. C., Noone, K. J., and Charlson, R. J.: Organic atmospheric aerosols: Review and state of science, Rev. Geophys., 38, 267-294, 2000.

Jafferson, A., Tanner, D. J., Eisele, F. L., Davis, D. D., Chen, G., Creawford, J., Huey, J. W., Torres, A. L., and Berresheim, H.: OH photochemistry and methane sulfonic acid formation in the coastal Antarctic boundary layer, J. Geophys. Res., 103, 1647-1656, 1998.

Kalberer, M., Yu, J., Cocker, D. R., Flagan, R. C., and Seinfeld, J. H.: Aerosol formation in the cyclohexene-ozone system, Environ. Sci. Technol., 34, 4894- 4901, 2000.

Kanakidou, M., Seinfeld, J. H., Pandis, S. N., Barnes, I., Dentener, F. J., Facchini, M. C., Van Dingenen, R., Ervens, B., Nenes, A., Nielsen, C. J., Swietlicki, E., Putaud, J. P., Balkanski, Y., Fuzzi, S., Horth, J., Moortgat, G. K., Winterhalter, R., Myhre, C. E. L., Tsigaridis, K., Vignati, E., Stephanou, E. G., and Wilson, J.: Organic aerosol and global climate modelling: a review, Atmos. Chem. Phys., 5, 1053-1123, 2005.

Kaufman, Y. J. and Fraser, R. S.: The effect of smoke particles on clouds and climate forcing, Science, 277, 1636-1639, 1997.

Kawamura, K. and Gagosian, R. B.: Implications of ω-oxocarboxylic acids in the remote marine atmosphere for photo-oxidation of unsaturated fatty acids, Nature, 325, 330-332, 1987.

Kawamura, K. and Ikushima, K.: Seasonal changes in the distribution of dicarboxylic acids in the urban atmosphere, Environ. Sci. Technol., 27, 2227-2235, 1993.

Kawamura, K. and Kaplan, I. R.: Motor Exhaust Emissions as a Primary Source for Dicarboxylic-Acids in Los-Angeles Ambient Air, Environ. Sci. Technol., 21, 105-110, 1987.

Kawamura, K. and Sakaguchi, F.: Molecular distributions of water soluble dicarboxylic acids in marine aerosols over the Pacific Ocean including tropics, J. Geophys. Res., 104, 3501-3509, 1999.

Kawamura, K. and Usukura, K.: Distributions of low molecular weight dicarboxylic acids in the North Pacific aerosol samples, J. Oceanogr., 49, 271-283, 1993.

743 Kawamura, K., Imai, Y., and Barrie, L. A.: Photochemical production and loss of organic acids in
744 high Arctic aerosols during long-range transport and polar sunrise ozone depletion events,
745 Atmos. Environ., 39, 599-614, 2005.

746 Kawamura, K., Kasukabe, H., and Barrie, L. A.: Source and reaction pathways of dicarboxylic
747 acids, ketoacids and dicarbonyls in arctic aerosols: One year of observations, Atmos.
748 Environ., 30, 1709-1722, 1996.

749 Kawamura, K., Narukawa, M., Li, S. M., and Barrie, L. A.: Size distributions of dicarboxylic acids
750 and inorganic ions in atmospheric aerosols collected during polar sunrise in the Canadian high
751 Arctic, J. Geophys. Res., 112, D10307, doi:10.1029/2006JD008244, 2007.

752 Kawamura, K., Ng, L., and Kaplan, I. R., Determination of organic acids (C_1-C_{10}) in the
753 atmosphere, motor-exhausts and engine oils, Environ. Sci. Technol., 19, 1082-1086, 1985.

754 Kawamura, K. and Pavuluri, C.M.: New Directions: Need for better understanding of plastic waste
755 burning as inferred from high abundance of terephthalic acid in South Asian aerosols, Atmos.
756 Environ., 44, 5320-5321, 2011.

757 Kawamura, K. and Yasui, O.: Diurnal changes in the distribution of dicarboxylic acids,
758 ketocarboxylic acids and dicarbonyls in the urban Tokyo atmosphere, Atmos. Environ., 39,
759 1945-1960, 2005.

760 Kawamura, K. and Bikkina, S.: A review of dicarboxylic acids and related compounds in
761 atmospheric aerosols: Molecular distributions, sources and transformation, Atmos. Res., 170,
762 140-160, 2016.

763 Kawamura, K.: Identification of C_2-C_{10} ω-oxocarboxylic acids, pyruvic acid, and C_2-C_3 α-
764 dicarbonyls in wet precipitation and aerosol samples by capillary GC and GC/MS, Anal.
765 Chem., 65, 3505-3511, 1993.

766 Kerminen, V. -M., Pakkanen, T. A., and Hillamo, R. E.: Interactions between inorganic trace gases
767 and supermicrometer particles at a coastal site, Atmos. Environ., 31, 2753-2765, 1997a.

768 Kerminen, V. -M., Aurela, M., Hillamo, R. E., and Virkkula, A.: Formation of particualte MSA:
769 deductions from size distribution measurements in the Finnish Arctic, Tellus, 49b, 159-171,
770 1997b.

771 Kleeman, M. J. and Cass, G. R.: Effect of emissions control strategies on the size and composition
772 distribution of urban particulate air pollution, Environ. Sci. Technol., 33, 177-189, 1999.

773 Kouyoumdjian, H. and Saliba, N. A.: Mass concentration and ion composition of coarse and fine
774 particles in an urban area in Beirut: effect of calcium carbonate on the absorption of nitric and
775 sulfuric acids and the depletion of chloride, Atmos. Chem. Phys., 6, 1865-1877, 2006.

776 Kumar, A., Sarin, M. M., and Sudheer, A. K.: Mineral and anthropogenic aerosols in Arabian Sea-
777 atmospheric boundary layer: Sources and spatial variability, Atmos. Environ., 42, 5169-5181,
778 2008.

779 Kundu S., Kawamura, K., Andreae, T. W., Hoffer, A., and Andreae, M. O.: Molecular distributions
780 of dicarboxylic acids, ketocarboxylic acids and α-dicarbonyls in biomass burning aerosols:
781 implications for photochemical production and degradation in smoke layers, Atmos. Chem.
782 Phys., 10, 2209-2225, 2010.

Kunwar, B. and Kawamura, K.: Seasonal distribution and sources of low molecular weight dicarboxylic acids, ω-oxocarboxylic acids, pyruvic acid, α-dicarbonyls and fatty acids in ambient aerosols from subtropical Okinawa in the western Pacific Rim, Environ. Chem., 11, 673-689, 2014.

Legrand, M., Preunkert, S., Oliveira, T., Pio, C. A., Hammer, S., Gelencser, A., Kasper-Giebl, A., and Laj, P.: Origin of C_2-C_5 dicarboxylic acids in the European atmosphere inferred from year-round aerosol study conducted at a west-east transect, J. Geophys. Res., 112, D23S07, doi:10.1029/2006JD008019, 2007.

Lim, H. J., Carlton, A. G., and Turpin, B. J.: Isoprene forms secondary organic aerosol through cloud processing: Model simulations, Environ. Sci. Technol., 39, 4441-4446, 2005.

Lim, Y. B., Tan, Y., Perri, M. J., Seitzinger, S. P., and Turpin, B. J.: Aqueous chemistry and its role in secondary organic aerosol (SOA) formation, Atmos. Chem. Phys., 10, 10521-10539, 2010.

Liu, S. Z., Tao, S., Liu, W. X., Liu, Y. N., Dou, H., Zhao, J. Y., Wang, L. G., Wang, J. F., Tian, Z. F., and Gao, Y.: Atmospheric polycyclic aromatic hydrocarbons in north China: A winter-time study, Environ. Sci. Technol., 41, 8256-8261, 2007.

Matsunaga, S., Kawamura, K., Nakatsuka, T., and Ohkouchi, N.: Preliminary study on laboratory photochemical formation of low molecular weight dicarboxylic acids from unsaturated fatty acid (oleic acid), Res. Org. Geochem., 14, 19-25, 1999.

Mayol-Bracero, O. L., Guyon, P., Graham, B., Roberts, G., Andreae, M. O., Decesari, S., Facchini, M. C., Fuzzi, S., and Artaxo, P.: Water-soluble organic compounds in biomass burning aerosols over Amazonia - 2. Apportionment of the chemical composition and importance of the polyacidic fraction, J. Geophys. Res., 107, 8091, doi:10.1029/2001jd000522, 2002.

Meinardi, S., Simpson, I. J., Blake, N. J., Blake, D. R., and Rowland, E. S.: Dimethyl disulfide (DMDS) and dimethyl sulfide (DMS) emissions from biomass burning in Australia, Geophys. Res. Lett., 30, 1454, doi:10.1029/2003GL016967, 2003.

Mkoma, S. L., Kawamura, K., and Fu, P. Q.: Contributions of biomass/biofuel burning to organic aerosols and particulate matter in Tanzania, East Africa, based on analyses of ionic species, organic and elemental carbon, levoglucosan and mannosan, Atmos. Chem. Phys., 13, 10325-10338, 2013.

Miyazaki, Y., Kawamura, K., and Sawano, M.: Size distributions and chemical characterization of water-soluble organic aerosols over the western North Pacific in summer, J. Geophys. Res., 115, D23210, doi:10.1029/2010JD014439, 2010.

Miyazaki, Y., Kawamura, K., Jung, J., Furutani, H., and Uematsu, M.: Latitudinal distributions of organic nitrogen and organic carbon in marine aerosols over the western North Pacific, Atmos. Chem. Phys., 11, 3037-3049, 2011.

Mochida, M., Kawabata, A., Kawamura, K., Hatsushika, H., and Yamazaki, K.: Seasonal variation and origins of dicarboxylic acids in marine atmosphere over the western North Pacific, J. Geophys. Res., 108, 4193, doi:10.1029/2002JD002355, 2003b.

Mochida, M., Umemoto, N., Kawamura, K., and Uematsu, M.: Bimodal size distribution of C_2-C_4 dicarboxylic acids in the marine aerosols, Geophys. Res. Lett., 30, 1672, doi: 10.1029/2003GL017451, 2003a.

824 Mochida, M., Umemoto, N., Kawamura, K., Lim, H. J., and Turpin, B. J.: Bimodal size
825 distributions of various organic acids and fatty acids in the marine atmosphere: Influence of
826 anthropogenic aerosols, Asian dusts, and sea spray off the coast of East Asia, J. Geophys.
827 Res., 112, D15209, doi:10.1029/2006JD007773, 2007.

828 Myriokefalitakis, S., Tsigaridis, K., Mihalopoulos, N., Sciare, J., Nenes, A., Kawamura, K., Segers,
829 A., and Kanakidou, M.: In-cloud oxalae formation in the regional troposphere: a 3-D
830 modelling study, Atmos. Chem. Phys., 11, 5761-5782, 2011.

831 Nenes, A., Pandis, S. N., and Pilinis, C.: ISORROPIA: A new thermodynamic equilibrium model
832 for multiphase multicomponent inorganic aerosols, Aquat. Geochem., 4, 123-152, 1998.

833 Pakkanen, T. A., Loukkola, K., Korhonen, C. H., Aurela, M., Makela, T., Hillamo, R. E., Aarnio,
834 P., Koskentalo, T., Kousa, A., and Maenhaut, W.: Sources and chemical composition of
835 atmospheric fine and coarse particles in the Helsinki area, Atmos. Environ., 35, 5381-5391,
836 2001.

837 Pavuluri, C. M., Kawamura, K., Mihalopoulos, N., and Swaminathan, T.: Laboratory
838 photochemical processing of aqueous aerosols: formaion and degradation of dicarboxylic
839 acids, oxocarboxylic acids, and alpha-dicarbonyls, Atmos. Chem. Phys., 15, 7999-8012, 2015.

840 Pope, C. A. and Dockery, D. W.: Health effects of fine particulate air pollution: Lines that connect,
841 J. Air Waste Manage., 56, 709-742, 2006.

842 Pradeep Kumar, P., Broekhuizen, K., and Abbatt, J. P. D.: Organic acids as cloud condensation
843 nuclei: Laboratory studies of highly soluble and insoluble species, Atmos. Chem. Phys., 3,
844 509-520, 2003.

845 Quinn, P. K., Covert, D. S., Bates, T. S., Kapustin, V. N., Ramseybell, D. C., and Mcinnes, L. M.:
846 Dimethylsulfide cloud condensation nuclei climate system - relevant size-resolved
847 measurements of the chemical and physical-properties of atmospheric aerosol-particles, J.
848 Geophys. Res., 98, 10411-10427, 1993.

849 Ramanathan, V., Crutzen, P. J., Kiehl, J. T., and Rosenfeld, D.: Atmosphere - Aerosols, climate,
850 and the hydrological cycle, Science, 294, 2119-2124, 2001.

851 Schauer, J. J., Rogge, W. F., Hildemann, L. M., Mazurek, M. A., and Cass, G. R.: Source
852 apportionment of airborne particualte matter using organic compounds as tracers, Atmos.
853 Environ., 30, 3837-3855, 1996.

854 Seinfeld, J. H. and Pandis, S. N.: Atmospheric chemistry and physics: From air pollution to climate
855 change, 2nd edition, J. Wiley, New York, 2006.

856 Seinfeld, J. H. and Pandis, S. N.: Atmospheric Chemistry and Physics, John Wiley & Sons, New
857 York, 1998.

858 Seinfeld, J. H. and Pankow, J. F.: Organic atmospheric particulate material, Annu. Rev. Phys.
859 Chem., 54, 121-140, 2003.

860 Sempéré, R. and Kawamura, K.: Trans-hemispheric contribution of C_2-C_{10} α,ω-dicarboxylic acids,
861 and related polar compounds to water-soluble organic carbon in the western Pacific aerosols
862 in relation to photochemical oxidation reactions, Glob. Biogeochem. Cycle, 17, 1069,
863 doi:10.1029/2002GB001980, 2003.

Shimada, K., Shimida, M., Takami, A., Hasegawa, S., Akihiro, F., Arakaki, T., Izumi, W., and Hatakeyama, S.: Mode and place of origin of carbonaceous aerosols transported from East Asia to Cape Hedo, Okinawa, Japan, Aerosol Air. Qual. Res., 15, 799-813, 2015.

Simoneit, B. R. T., Medeiros, P. M., and Didyk, B. M.: Combustion products of plastics as indicators for refuse burning in the atmosphere, Environ. Sci. Technol., 39, 6961-6970, 2005.

Speer, R. E., Edney, E. O., and Kleindienst, T. E.: Impact of organic compounds on the concentrations of liquid water in ambient $PM_{2.5}$, J. Aerosol Sci., 34, 63-77, 2003.

Takami, A., Miyoshi, T., Shimono, A., Kaneyasu, N., Kato, S., Kajii, Y., and Hatakeyama, S.: Transport of anthropogenic aerosols from Asia and subsequent chemical transformation, J. Geophys. Res., 112, D22S31, doi 10.1029/2006jd008120, 2007.

Takiguchi, Y., Takami, A., Sadanaga, Y., Lun, X. X., Shimizu, A., Matsui, I., Sugimoto, N., Wang, W., Bandow, H., and Hatakeyama, S.: Transport and transformation of total reactive nitrogen over the East China Sea, J. Geophys. Res., 113, D10306, doi:10.1029/2007jd009462, 2008.

Tao, J., Zhang, L., Engling, G., Zhang, R., Yang, T., Cao, J., Zhu, C., Wang, Q., and Luo, L.: Chemical composition of $PM_{2.5}$ in an urban environment in Chengdu, China: Importance of springtime dust storms and biomass burning, Atmos. Res., 122, 270-283, 2013.

Tao, S., Wang, Y., Wu, S. M., Liu, S. Z., Dou, H., Liu, Y. N., Lang, C., Hu, F., and Xing, B. S.: Vertical distribution of polycyclic aromatic hydrocarbons in atmospheric boundary layer of Beijing in winter, Atmos. Environ., 41, 9594-9602, 2007.

Tedetti, M., Kawamura, K., Narukawa, M., Joux, F., Charriere, B., and Sempéré, R.: Hydroxyl radical-induced photochemical formation of dicarboxylic acids from unsaturated fatty acid (oleic acid) in aqueous solution, J. Photochem. Photobiol A., 188, 135-139, 2007.

Tsai, Y. I. and Chen, C. L.: Characterization of Asian dust storm and non-Asian dust storm $PM_{2.5}$ aerosol in southern Taiwan, Atmos. Environ., 40, 4734-4750, 2006.

Turpin, B. J. and Lim, H. J.: Species contributions to $PM_{2.5}$ mass concentrations: Revisiting common assumptions for estimating organic mass, Aerosol. Sci. Tech., 35, 602-610, 2001.

Volkamer, R., Platt, U., and Wirtz, K.: Primary and secondary glyoxal formation from aromatics: Experimental evidence for the bicycloalkyl-radical pathway from benzene, toluene, and p-xylene, J. Phys. Chem. A, 105, 7865-7874, 2001.

Wang, G. H., Kawamura, K., Xie, M. J., Hu, S. Y., Li, J. J., Zhou, B. H., Cao, J. J., and An, Z. S.: Selected water-soluble organic compounds found in size-resolved aerosols collected from urban, mountain and marine atmospheres over East Asia, Tellus, 63, 371-381, 2011.

Wang, G. H., Zhao, B. H., Cheng, C. L., Cao, J. J., Li, J. J., Meng, J. J., Tao, J., Zhang, R. J., and Fu, P. Q.: Impact of Gobi desert dust on aerosol chemistry of Xi'an, inland China during spring 2009: differences in composition and size distribution between the urban ground surface and the mountain atmosphere, Atmos. Chem. Phys., 13, 819-835, 2013.

Wang, H., Kawamura, K., and Shooter, D.: Carbonaceous and ionic components in wintertime atmospheic aeosols from two New Zwaland cities: Implication for solid fuel combustion, Atmos. Environ., 39, 5865-5875, 2005a.

903 Wang, Y., Zhuang, G. S., Sun, Y., and An, Z. S.: Water-soluble part of the aerosol in the dust storm
904 season - evidence of the mixing between mineral and pollution aerosols, Atmos. Environ., 39,
905 7020-7029, 2005b.

906 Warneck, P.: In-cloud chemistry opens pathway to the formation of oxalic acid in the marine
907 atmosphere, Atmos. Environ., 37, 2423-2427, 2003.

908 Yamasoe, M. A., Artaxo, P., Miguel, A. H., and Allen, A. G.: Chemical composition of aerosol
909 particles from direct emissions of vegetation fires in the Amazon Basin: water-soluble species
910 and trace elements, Atmos. Environ., 34, 1641-1653, 2000.

911 Ziemann, P. J.: Aerosol products, mechanisms, and kinetics of heterogeneous reactions with oleic
912 acid in pure and mixed particles, Faraday Discuss., 130, 469-490, 2005.

913 Zimmermann, J. and Poppe, D.: A supplement for the RADM2 chemical mechanism: The
914 photooxidation of isoprene, Atmos. Environ., 30, 1255-1269, 1996.

Table 1. Concentrations (μg m^{-3}) of major inorganic ions and carbonaceous species in the fine and coarse mode aerosols in Okinawa Island in the Western North Pacific.

Inorganic ions	Fine mode[a]				Coarse mode[b]			
	Mean	S.D.[c]	Min.[d]	Max.[e]	Mean	S.D.	Min.	Max.
	Water-soluble inorganic ions							
	Cations							
Na^+	0.44	0.20	0.21	0.72	2.42	0.89	1.60	3.65
NH_4^+	2.40	1.18	0.74	3.69	0.03	0.01	0.03	0.05
K^+	0.14	0.06	0.04	0.21	0.09	0.02	0.07	0.12
Mg^{2+}	0.07	0.02	0.04	0.10	0.34	0.11	0.24	0.49
Ca^{2+}	0.06	0.02	0.04	0.09	0.41	0.19	0.15	0.60
Total cations	3.12	1.22	1.28	4.37	3.29	1.02	2.55	4.82
	Anions							
MSA^-	0.04	0.01	0.03	0.06	0.01	0.00	0.00	0.01
Cl^-	0.12	0.13	0.02	0.29	4.27	2.25	1.77	7.25
NO_3^-	0.14	0.08	0.04	0.23	1.61	0.54	0.94	2.41
SO_4^{2-}	10.1	4.85	2.88	14.9	1.46	0.44	0.69	1.81
Total anions	10.4	4.73	3.33	15.1	7.35	2.20	5.69	10.6
	Total water-soluble ions							
Total water-soluble ions	13.5	5.95	4.61	19.5	10.6	3.22	8.33	15.4
	Carbonaceous components							
WSOC	1.12	0.49	0.31	1.61	0.33	0.13	0.15	0.52
OC	1.62	0.59	0.62	2.12	0.60	0.17	0.36	0.82
OM	3.43	1.31	1.30	4.87	1.25	0.36	0.75	1.73
EC	0.05	0.03	0.00	0.09	-	-	-	-
TC	1.67	0.65	0.62	2.41	0.60	0.17	0.36	0.82

[a]Fine mode represents aerosol size of $D_p < 2.1$ μm.
[b]Coarse mode represents aerosol size of $D_p > 2.1$ μm.
[c]Standard deviation.
[d]Minimum.
[e]Maximum.

Table 2. Summarized concentrations (ng m^{-3}) of water-soluble dicarboxylic acids and related polar compounds in the fine and coarse mode aerosols from Okinawa Island in the western North Pacific Rim.

Compounds	Abbreviation	Chemical formula	Fine mode[a]				Coarse mode[b]			
			Mean	S.D.[c]	Min.[d]	Max.[e]	Mean	S.D.	Min.	Max.
			Dicarboxylic acids							
Saturated normal-chain diacids										
Oxalic	C_2	HOOC-COOH	135	37.4	76.0	176	40.2	14.7	22.1	60.0
Malonic	C_3	HOOC-CH_2-COOH	19.5	6.84	7.56	23.6	12.4	3.52	6.87	15.5
Succinic	C_4	HOOC-$(CH_2)_2$-COOH	13.4	4.98	5.08	17.5	8.02	2.21	4.66	10.1
Glutaric	C_5	HOOC-$(CH_2)_3$-COOH	3.30	1.54	1.00	4.75	1.89	0.57	1.07	2.66
Adipic	C_6	HOOC-$(CH_2)_4$-COOH	3.49	1.09	2.47	4.98	2.50	1.24	1.45	4.23
Pimelic	C_7	HOOC-$(CH_2)_5$-COOH	0.46	0.24	0.04	0.63	0.32	0.11	0.20	0.44
Suberic	C_8	HOOC-$(CH_2)_6$-COOH	0.07	0.07	0.00	0.16	0.04	0.02	0.02	0.07
Azelaic	C_9	HOOC-$(CH_2)_7$-COOH	1.20	0.72	0.51	2.41	1.15	0.60	0.49	2.10
Decanedioic	C_{10}	HOOC-$(CH_2)_8$-COOH	0.17	0.11	0.01	0.30	0.08	0.07	0.03	0.19
Undecanedioic	C_{11}	HOOC-$(CH_2)_9$-COOH	0.47	0.33	0.13	0.76	0.25	0.10	0.14	0.38
Dodecanedioic	C_{12}	HOOC-$(CH_2)_{10}$-COOH	0.07	0.03	0.03	0.09	0.05	0.02	0.02	0.07
Branched-chain diacids										
Methylmalonic	iC_4	HOOC-CH(CH_3)-COOH	0.43	0.23	0.09	0.71	0.47	0.37	0.09	0.99
Methylsuccinic	iC_5	HOOC-CH(CH_3)-COOH	0.81	0.27	0.37	1.00	0.59	0.13	0.45	0.80
2-Methylglutaric	iC_6	HOOC-CH(CH_3)-$(CH_2)_2$-COOH	0.35	0.24	0.05	0.70	0.19	0.20	0.04	0.53
Unsaturated aliphatic diacids										
Maleic	M	HOOC-CH=CH-COOH - *cis*	0.81	0.25	0.41	1.05	0.73	0.23	0.37	0.95
Fumaric	F	HOOC-CH=CH-COOH - *trans*	0.31	0.09	0.20	0.42	0.21	0.08	0.12	0.30
Methylmaleic	mM	HOOC-C(CH_3)=CH-COOH - *cis*	0.34	0.27	0.11	0.76	0.57	0.48	0.11	1.37
Unsaturated aromatic diacids										
Phthalic	Ph	HOOC-(C_6H_4)-COOH - *o-isomer*	6.29	2.85	1.99	9.3	2.79	0.81	1.85	3.9
Isophthalic	iPh	HOOC-(C_6H_4)-COOH - *m-isomer*	0.46	0.07	0.35	0.55	0.17	0.06	0.09	0.22
Terephthalic	tPh	HOOC-(C_6H_4)-COOH - *p-isomer*	2.21	1.15	0.32	3.30	0.64	0.38	0.09	1.17
Multifunctional diacids										
Malic	hC_4	HOOC-CH(OH)-CH_2-COOH	0.14	0.05	0.11	0.21	0.14	0.06	0.07	0.20
Ketomalonic	kC_3	HOOC-C(O)-COOH	4.92	3.79	0.46	9.28	0.49	0.17	0.32	0.77
4-Ketopimelic	kC_7	HOOC-CH_2-CH_2-HC(O)$(CH_2)_2$-COOH	2.57	0.83	1.26	3.20	0.43	0.16	0.26	0.69
Total diacids			196	58.1	98.3	253	74.1	24.3	41.4	105
			ω-Oxocarboxylic acids							
Glyoxylic	ωC_2	OHC-COOH	14.1	5.92	4.77	20.2	4.81	2.00	2.23	7.20
3-Oxopropanoic	ωC_3	OHC-CH_2-COOH	0.08	0.05	0.00	0.12	0.05	0.04	0.02	0.12
4-Oxobutanoic	ωC_4	OHC-$(CH_2)_2$-COOH	2.23	1.12	0.86	3.56	0.68	0.35	0.41	1.22
9-Oxononanoic	ωC_9	OHC-$(CH_2)_7$-COOH	0.74	0.20	0.54	1.07	1.06	0.34	0.57	1.41
Total oxoacids			17.1	7.04	6.27	25.0	6.60	2.33	3.26	9.52
			Ketoacid							
Pyruvic	Pyr	CH_3-C(O)-COOH	2.61	0.76	1.67	3.48	2.32	1.20	0.76	4.09
			α-Dicarbonyls							
Glyoxal	Gly	OHC-CHO	2.74	1.12	1.45	4.40	0.84	0.26	0.50	1.17
Methylglyoxal	MeGly	CH_3-C(O)-CHO	1.09	0.98	0.25	2.53	0.65	0.16	0.45	0.87
Total α-dicarbonyls			2.83	1.59	1.03	4.68	1.49	0.37	0.96	1.86
			Aromatic monoacid							
Benzoic acid		C_6H_5-COOH	16.5	11.0	4.57	28.3	1.98	1.01	0.70	3.38

[a]Fine mode represents aerosol size of $D_p < 2.1$ μm.
[b]Coarse mode represents aerosol size of $D_p > 2.1$ μm.
[c]Standard deviation.
[d]Minimum.
[e]Maximum.

Table 3. Pearson correlation coefficients[a] (*r*) matrix among the selected chemical species/components measured in the fine and coarse mode aerosols from Okinawa Island in the western North Pacific Rim.

	Fine mode[b]																				
	Na^+	NH_4^+	K^+	Mg^{2+}	Ca^{2+}	MSA^-	Cl^-	NO_3^-	SO_4^{2-}	WSOC	OC	C_2	C_3	C_4	C_5	C_9	Ph	ωC_2	ωC_9	Gly	Benzoic	LWC
Na^+	1.00																					
NH_4^+	-0.25	1.00																				
K^+	-0.32	0.99	1.00																			
Mg^{2+}	0.98	-0.16	-0.23	1.00																		
Ca^{2+}	-0.21	0.62	0.33	-0.15	1.00																	
MSA^-	-0.32	0.92	0.92	-0.17	0.53	1.00																
Cl^-	0.65	-0.85	-0.85	0.58	-0.33	-0.78	1.00															
NO_3^-	0.65	-0.56	-0.55	0.68	0.22	-0.36	0.76	1.00														
SO_4^{2-}	-0.10	0.99	0.98	-0.02	0.59	0.89	-0.78	-0.49	1.00													
WSOC	0.10	0.91	0.93	0.16	0.30	0.79	-0.57	-0.27	0.96	1.00												
OC	0.12	0.91	0.95	0.16	0.25	0.80	-0.57	-0.32	0.93	0.99	1.00											
C_2	0.12	0.89	0.85	-0.13	0.22	0.80	-0.53	-0.30	0.92	0.99	0.98	1.00										
C_3	-0.05	0.90	0.89	-0.05	0.20	0.66	-0.68	-0.53	0.90	0.93	0.96	0.89	1.00									
C_4	-0.12	0.96	0.95	-0.09	0.15	0.76	-0.75	-0.55	0.96	0.95	0.96	0.92	0.99	1.00								
C_5	-0.12	0.99	0.96	-0.05	0.33	0.87	-0.80	-0.53	0.99	0.93	0.93	0.91	0.95	0.97	1.00							
C_9	0.64	0.01	0.02	0.61	0.42	-0.16	0.46	0.47	0.10	0.20	0.39	0.38	0.33	0.23	0.09	1.00						
Ph	0.41	0.78	0.73	0.46	0.42	0.63	-0.40	-0.16	0.87	0.92	0.93	0.90	0.83	0.83	0.86	0.23	1.00					
ωC_2	0.11	0.92	0.90	0.19	0.19	0.82	-0.57	-0.25	0.96	0.99	0.99	0.99	0.90	0.93	0.95	0.36	0.93	1.00				
ωC_9	0.23	0.22	0.12	0.18	-0.56	-0.01	-0.32	-0.53	0.29	0.13	0.22	0.05	0.31	0.26	0.32	0.80	0.02	0.16	1.00			
Gly	0.01	0.86	0.86	0.15	0.09	0.92	-0.52	-0.07	0.86	0.89	0.82	0.93	0.70	0.78	0.85	0.21	0.85	0.92	-0.11	1.00		
Benzoic	-0.13	0.99	0.99	-0.05	-0.23	0.90	-0.27	0.46	0.99	0.96	0.99	0.93	0.91	0.96	0.99	0.12	0.85	0.96	0.21	0.90	1.00	
LWC	0.16	0.87	0.83	0.30	0.53	0.88	-0.53	-0.13	0.92	0.90	0.87	0.92	0.82	0.83	0.89	0.18	0.90	0.95	0.19	0.95	0.91	1.00
	Coarse mode[c]																					
	Na^+	NH_4^+	K^+	Mg^{2+}	Ca^{2+}	MSA^-	Cl^-	NO_3^-	SO_4^{2-}	WSOC	OC	C_2	C_3	C_4	C_5	C_9	Ph	ωC_2	ωC_9	Gly	Benzoic	LWC
Na^+	1.00																					
NH_4^+	0.60	1.00																				
K^+	0.96	0.77	1.00																			
Mg^{2+}	0.98	0.63	0.33	1.00																		
Ca^{2+}	-0.12	0.03	-0.06	-0.29	1.00																	
MSA^-	-0.15	-0.66	-0.03	-0.25	-0.02	1.00																
Cl^-	0.98	0.59	0.90	0.98	-0.27	-0.22	1.00															
NO_3^-	-0.30	-0.23	-0.15	-0.39	0.98	0.28	-0.55	1.00														
SO_4^{2-}	0.33	0.32	0.56	0.28	0.63	0.25	0.16	0.67	1.00													
WSOC	-0.18	-0.26	0.06	-0.20	0.23	0.55	-0.36	0.92	0.72	1.00												
OC	-0.11	-0.10	0.13	-0.10	0.21	0.36	-0.28	0.92	0.72	0.97	1.00											
C_2	-0.05	0.26	0.30	0.15	0.63	0.09	-0.08	0.88	0.76	0.93	0.82	1.00										
C_3	0.32	0.33	0.53	0.31	0.68	0.18	0.15	0.75	0.92	0.88	0.82	0.93	1.00									
C_4	0.33	0.39	0.60	0.35	0.53	0.16	0.33	0.32	0.88	0.31	0.55	0.36	0.63	1.00								
C_5	0.05	0.05	0.22	-0.06	0.62	0.32	-0.05	0.43	0.75	0.28	0.38	0.22	0.45	0.91	1.00							
C_9	0.85	0.20	0.25	0.91	-0.16	-0.59	0.85	-0.31	0.18	-0.08	-0.25	0.25	0.30	0.19	-0.23	1.00						
Ph	-0.52	-0.54	-0.29	-0.54	0.73	0.59	-0.66	0.93	0.54	0.56	0.33	0.63	0.58	0.21	0.40	-0.58	1.00					
ωC_2	0.23	0.37	0.85	0.68	0.12	0.42	0.59	0.23	0.73	0.53	0.52	0.53	0.76	0.60	0.32	0.23	0.21	1.00				
ωC_9	0.83	0.53	0.82	0.87	-0.33	0.03	0.80	-0.22	0.21	0.07	0.16	0.28	0.38	0.08	-0.31	0.93	-0.28	0.33	1.00			
Gly	0.26	0.26	0.78	0.57	0.05	0.52	0.58	0.06	0.69	0.28	0.33	0.22	0.55	0.76	0.57	0.24	0.12	0.89	0.13	1.00		
Benzoic	-0.40	-0.60	-0.57	-0.36	-0.70	0.17	-0.29	-0.43	-0.88	-0.40	-0.35	-0.57	-0.73	-0.91	-0.77	-0.37	0.19	-0.48	-0.07	-0.51	1.00	
LWC	0.61	0.03	0.53	0.56	-0.70	0.48	0.63	-0.51	-0.10	-0.19	-0.13	-0.29	-0.08	-0.03	-0.22	0.23	-0.31	0.57	0.25	0.63	0.31	1.00

See Table 1 and 2 for abbreviation.

[a]Correlation is significant at 0.05 level for the values where *r* is > 0.80.

[b]Fine mode represents aerosol size of $D_p < 2.1$ μm.

[c]Coarse mode represents aerosol size of $D_p > 2.1$ μm.

915 **Figure Captions**

916 **Figure 1.** A map of East Asia with the location of Okinawa Island (26.87°N and 128.25°E) and
917 Asian countries.

918 **Figure 2.** Seven-day backward air mass trajectories (NOAA HYSPLIT) at 500 m a.g.l. (0900 UTC)
919 for the aerosol samples (OKI-1 to OKI-5) collected in Okinawa Island. The dates given in each
920 panel are the starting and ending times of collection of aerosol samples in Okinawa Island. Color
921 scale shows the altitude of the air parcel.

922 **Figure 3.** Average molecular distributions of water-soluble dicarboxylic acids and related
923 compounds in size-segregated aerosols collected in Okinawa Island.

924 **Figure 4.** Size distributions of water-soluble inorganic ions in the aerosol samples collected in
925 Okinawa Island.

926 **Figure 5.** Size distributions of selected water-soluble dicarboxylic acids and related compounds in
927 the aerosol samples collected in Okinawa Island.

928 **Figure 6.** Size distributions of water-soluble organic carbon (WSOC) and organic carbon (OC) in
929 the aerosol samples collected in Okinawa Island.

930 **Figure 7.** Aerosol liquid water contents for each sample in size-segregated aerosols and average
931 liquid water contents in size-segregated aerosols in Okinawa Island.

932 **Figure 8.** Mass concentration ratios of malonic to succinic acid and phthalic to azelaic acid in size-
933 segregated aerosols collected in Okinawa Island.

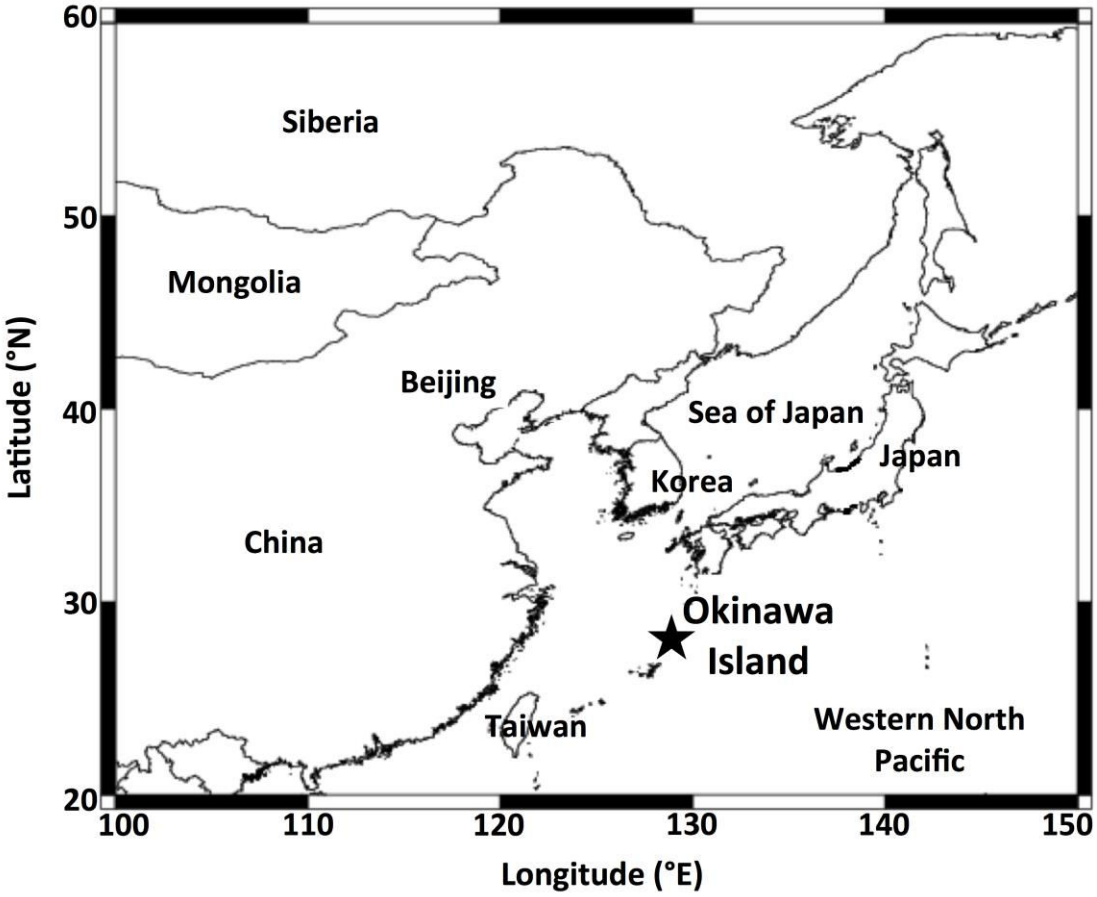

934

935 **Figure 1.** A map of East Asia with the location of Okinawa Island (26.87°N and 128.25°E) and

936 Asian countries.

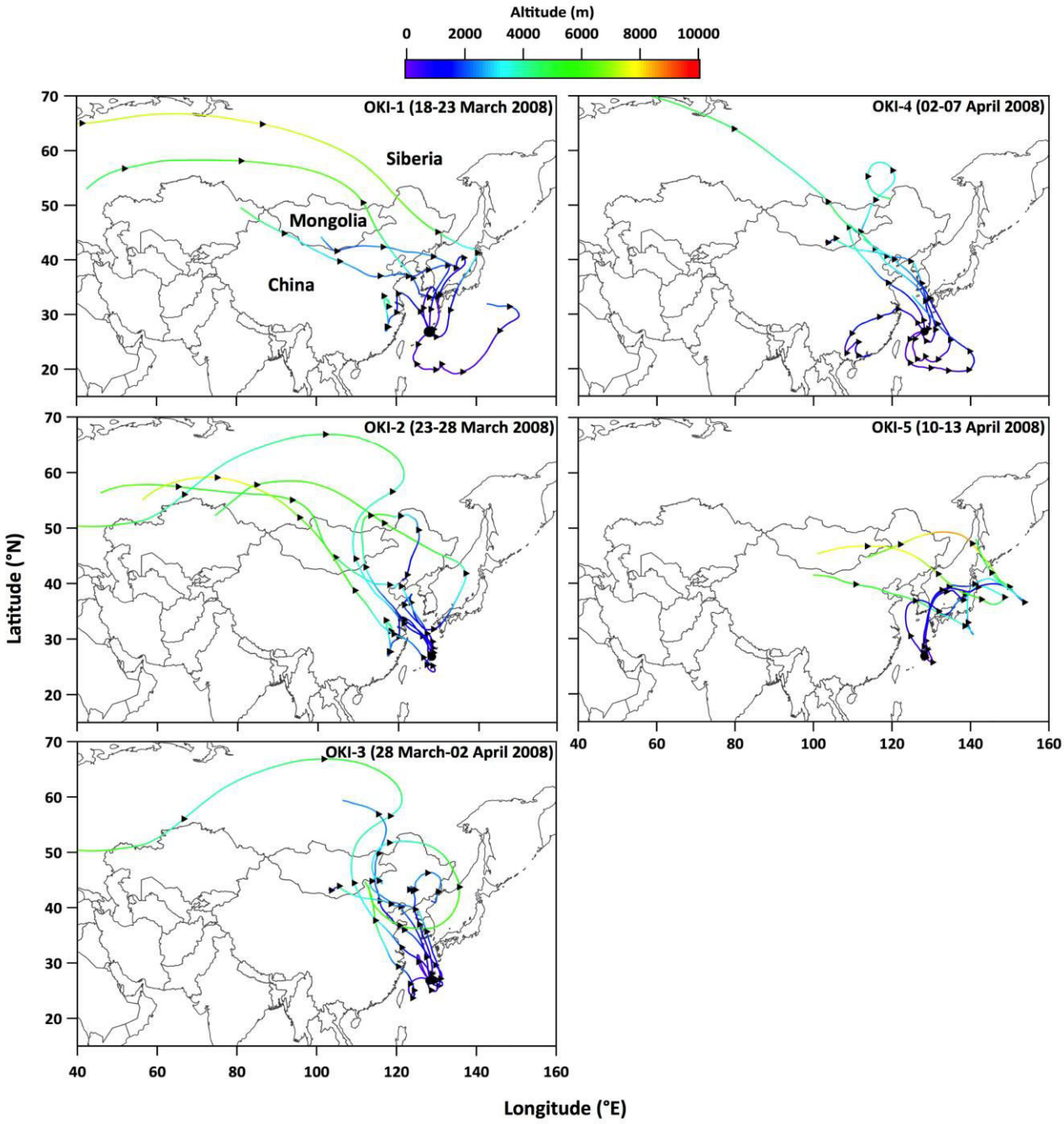

937

938 **Figure 2.** Seven-day backward air mass trajectories (NOAA HYSPLIT) at 500 m a.g.l. (0900 UTC)
939 for the aerosol samples (OKI-1 to OKI-5) collected in Okinawa Island. The dates given in each
940 panel are the starting and ending times of the collection of aerosol samples in Okinawa Island.
941 Color scale shows the altitude of the air parcel.

942

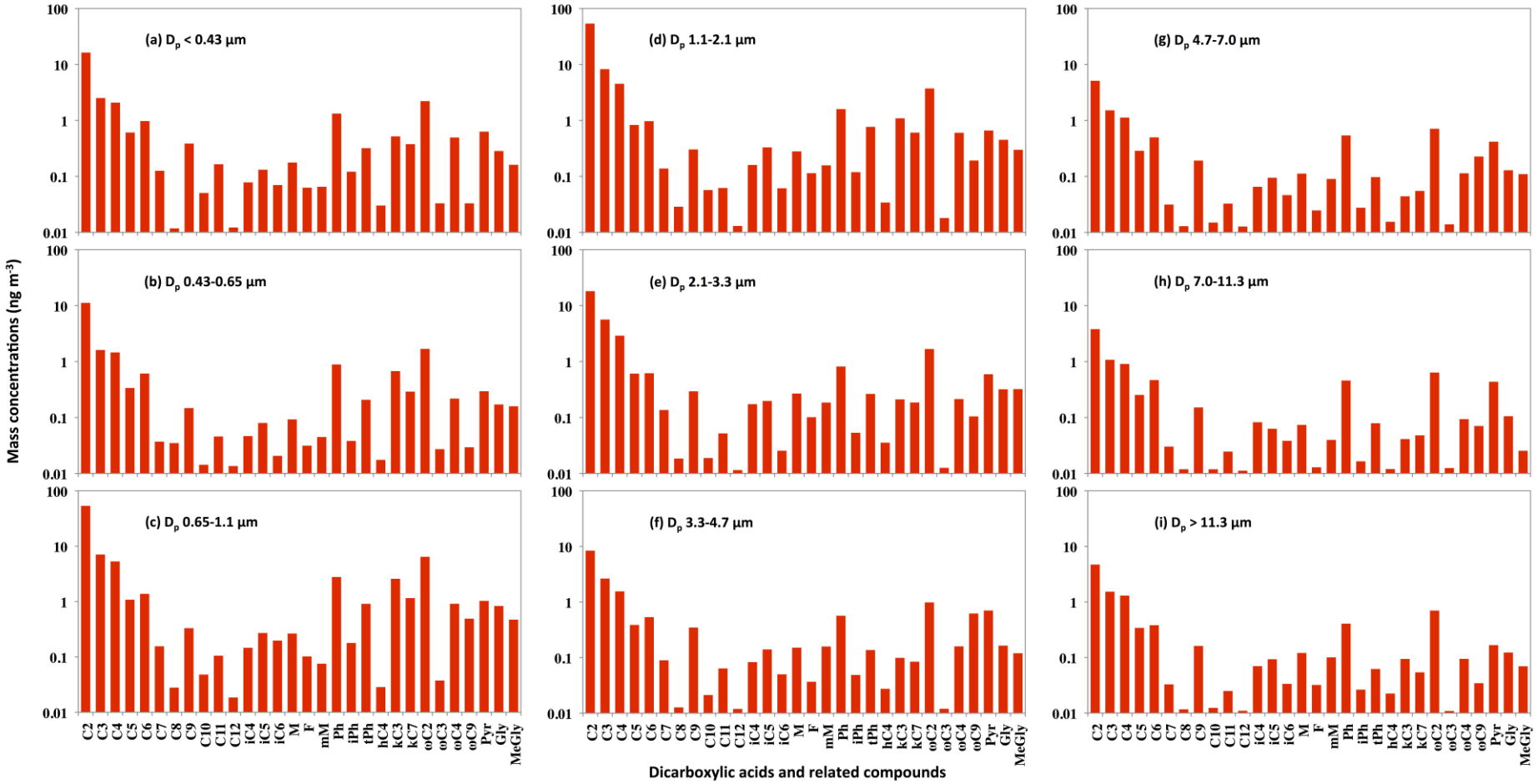

943

944 **Figure 3.** Average molecular distributions of water-soluble dicarboxylic acids and related compounds in size-segregated aerosols collected in Okinawa

945 Island.

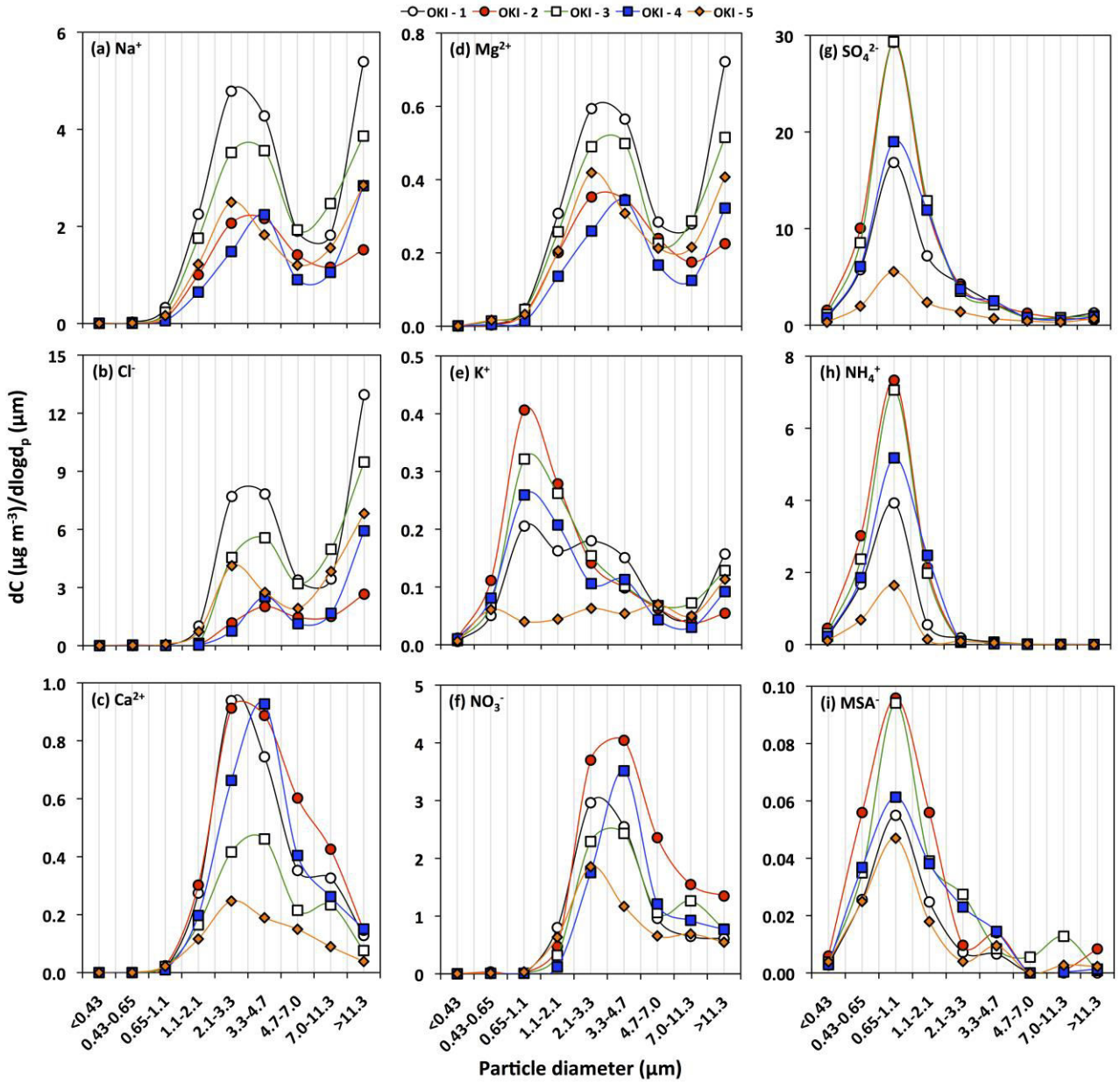

946

947 **Figure 4.** Size distributions of water-soluble inorganic ions in the aerosol samples collected in

948 Okinawa Island.

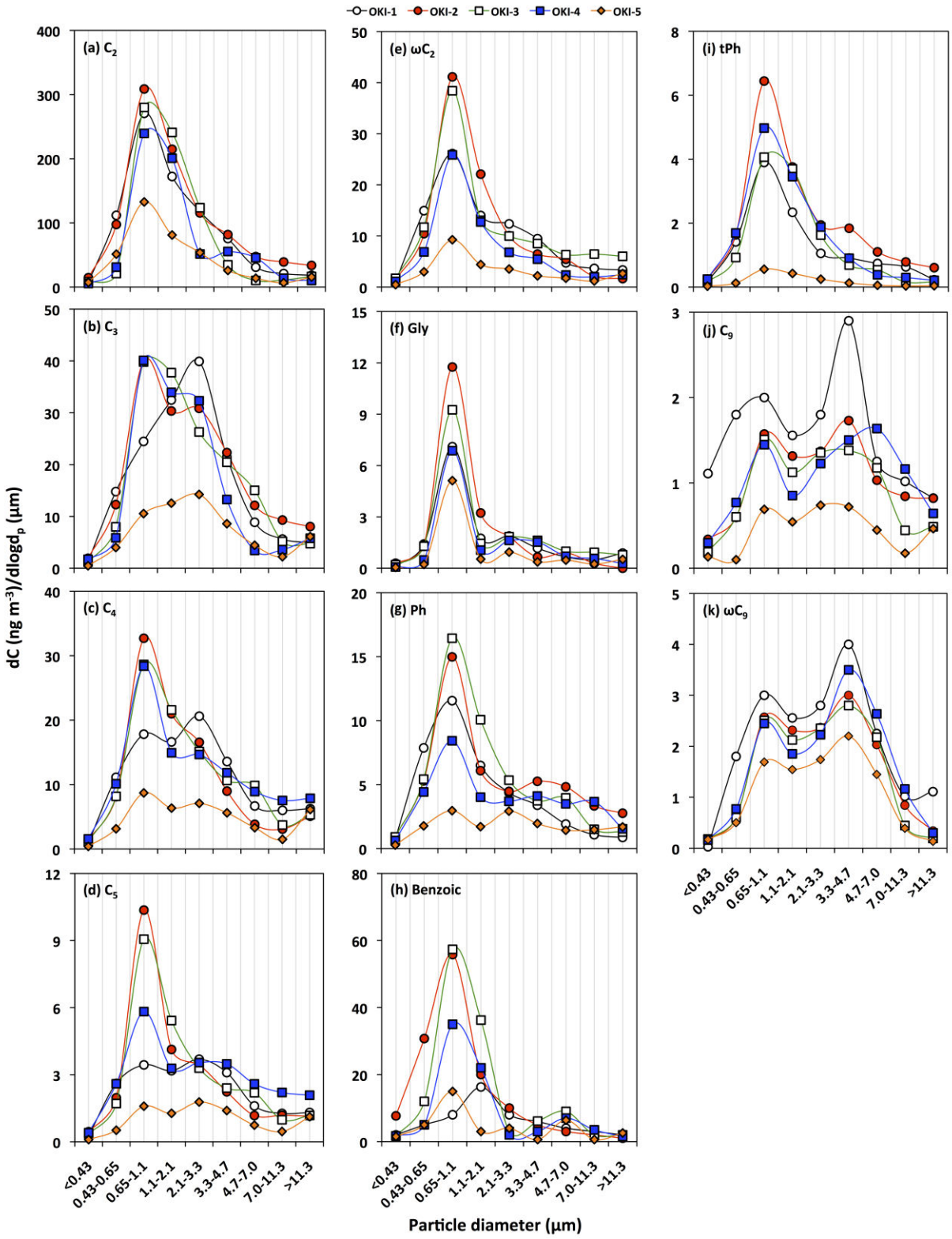

949

950 **Figure 5.** Size distributions of selected water-soluble dicarboxylic acids and related compounds in

951 the aerosol samples collected in Okinawa Island.

952

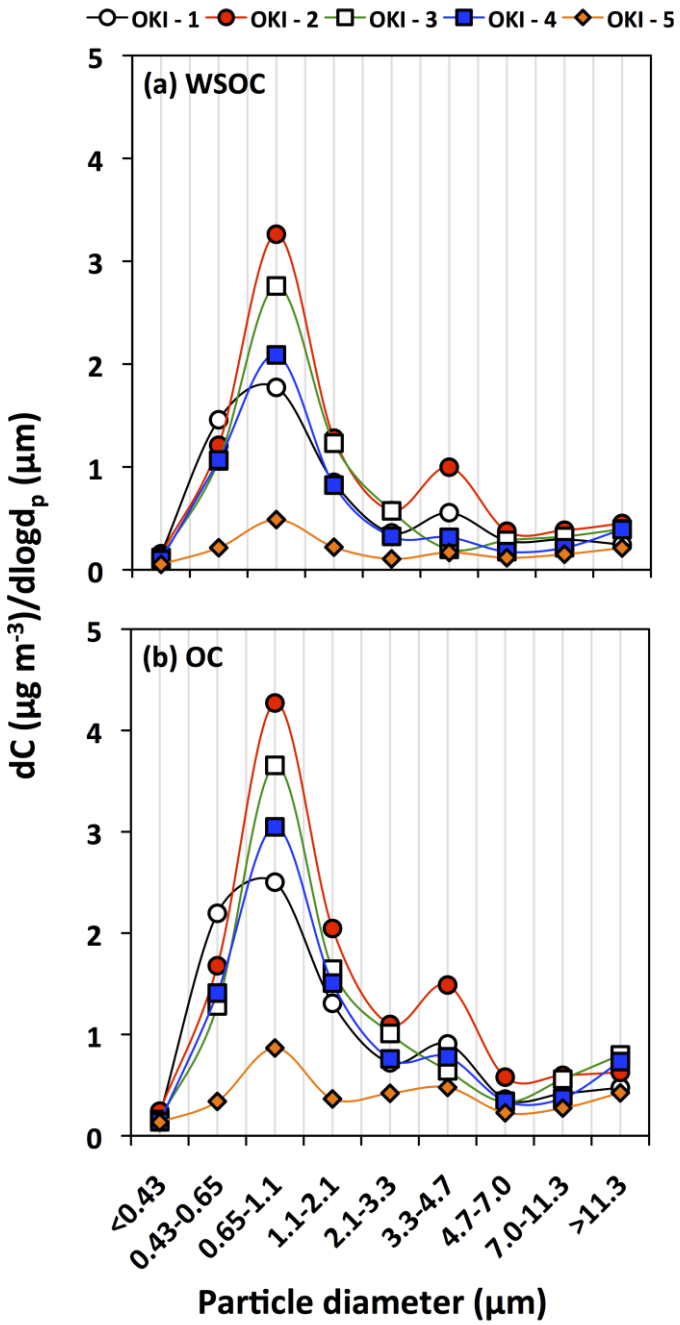

953

954 **Figure 6.** Size distributions of water-soluble organic carbon (WSOC) and organic carbon (OC) in

955 the aerosol samples collected in Okinawa Island.

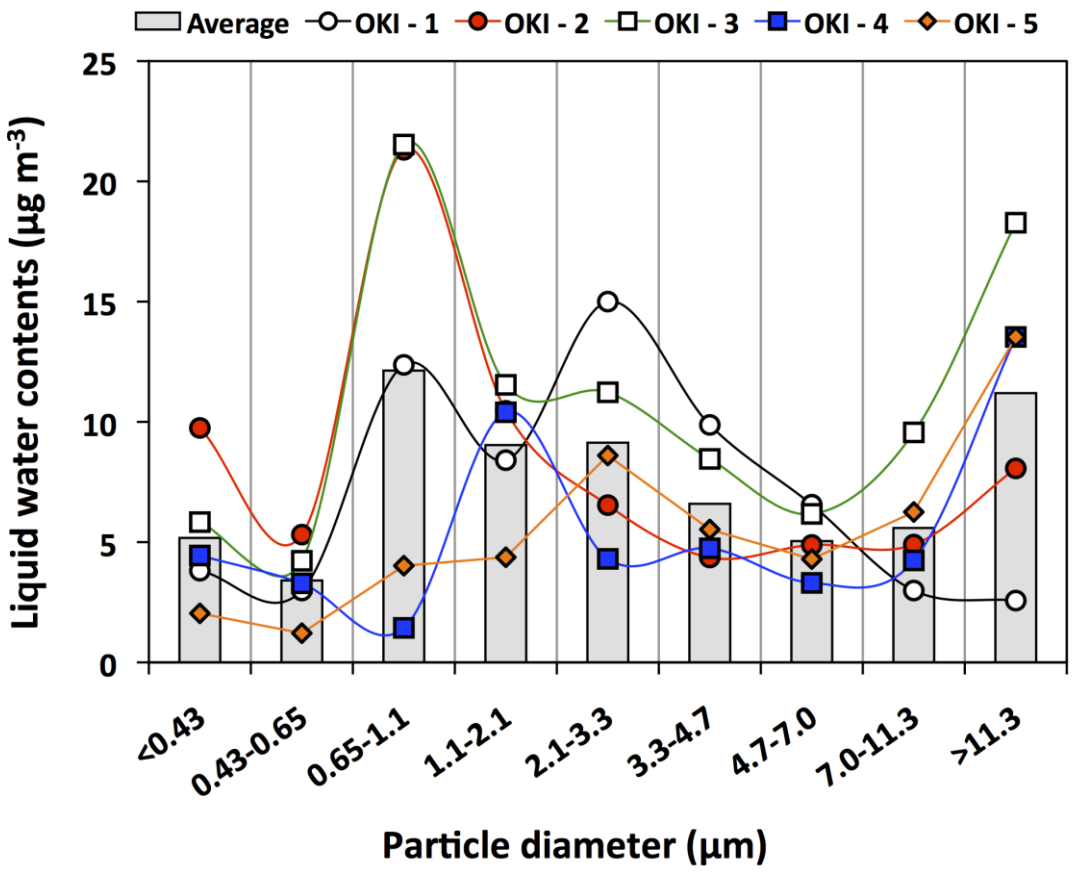

956

957 **Figure 7.** Aerosol liquid water contents for each sample in size-segregated aerosols and average

958 liquid water contents in size-segregated aerosols in Okinawa Island.

959

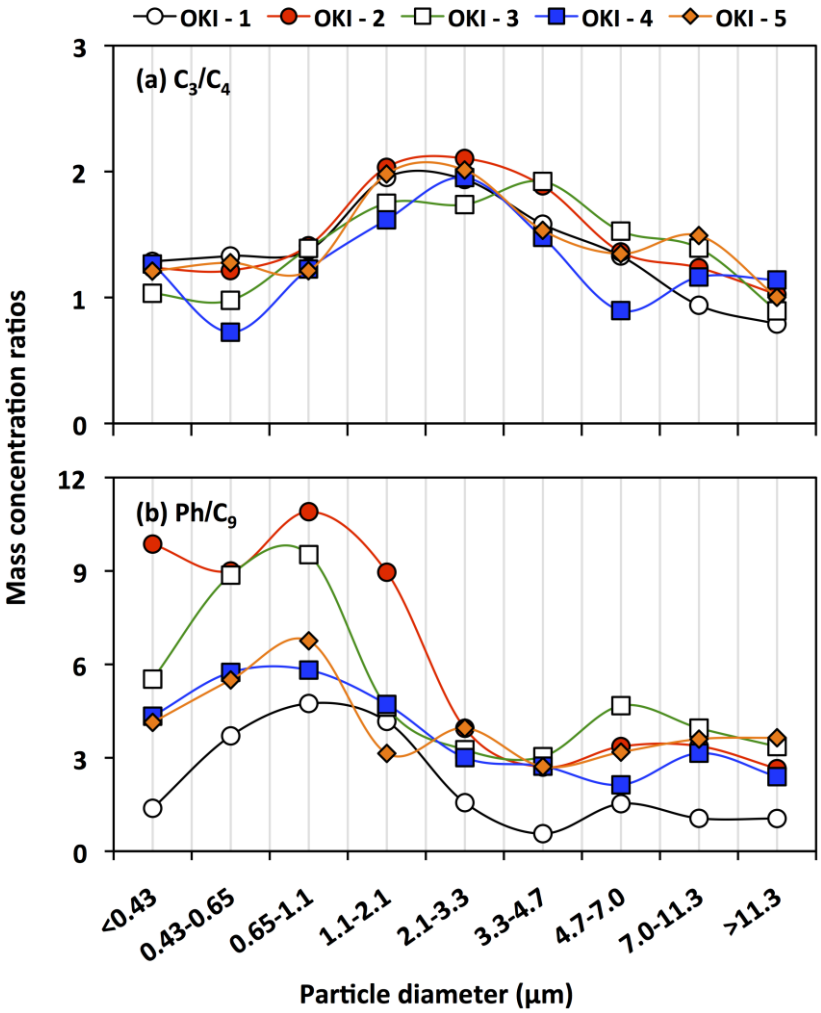

960

961 **Figure 8.** Mass concentration ratios of malonic to succinic acid and phthalic to azelaic acid in size-

962 segregated aerosols collected in Okinawa Island.

Supporting Information of

Dicarboxylic acids, oxoacids, benzoic acid, α-dicarbonyls, WSOC, OC, and ions in spring aerosols from Okinawa Island in the western North Pacific Rim: Size distributions and formation processes

D. K. Deshmukh et al.

This file includes:

Figures:

Figure S1. Seven-day backward air mass trajectories (NOAA HYSPLIT) at 500 m a.g.l. corresponding to 0900 UTC for the aerosol samples collected (OKI-1 to OKI-5) in Okinawa Island. The dates along with the sample ID are the starting and ending times for the collection of aerosol samples in Okinawa Island.

Figure S2. Seven-day backward air mass trajectories (NOAA HYSPLIT) at 500 m a.g.l. (0900 UTC) along with the data of (a) precipitation and (b) downward solar radiation flux for the aerosol samples collected (OKI-1 to OKI-5) in Okinawa Island. The dates given in each panel in figure are the starting and ending times of collection of aerosol samples in Okinawa Island.

Figure S3. The scatter plots of C_2 with C_3-C_5 diacids, ωC_2 and Gly in fine and coarse mode aerosols in Okinawa.

Tables:

Table S1. Correlation coefficient (r) and slope of the linear regression of oxalic acid (C_2) with other diacids and related compounds together with their statistical significance between fine and coarse mode aerosols in Okinawa Island.

Table S2. Correlation coefficient (r) and slope of the linear regression of oxalic acid (C_2) with other diacids and related compounds together with their statistical significance in fine mode aerosols in Okinawa Island.

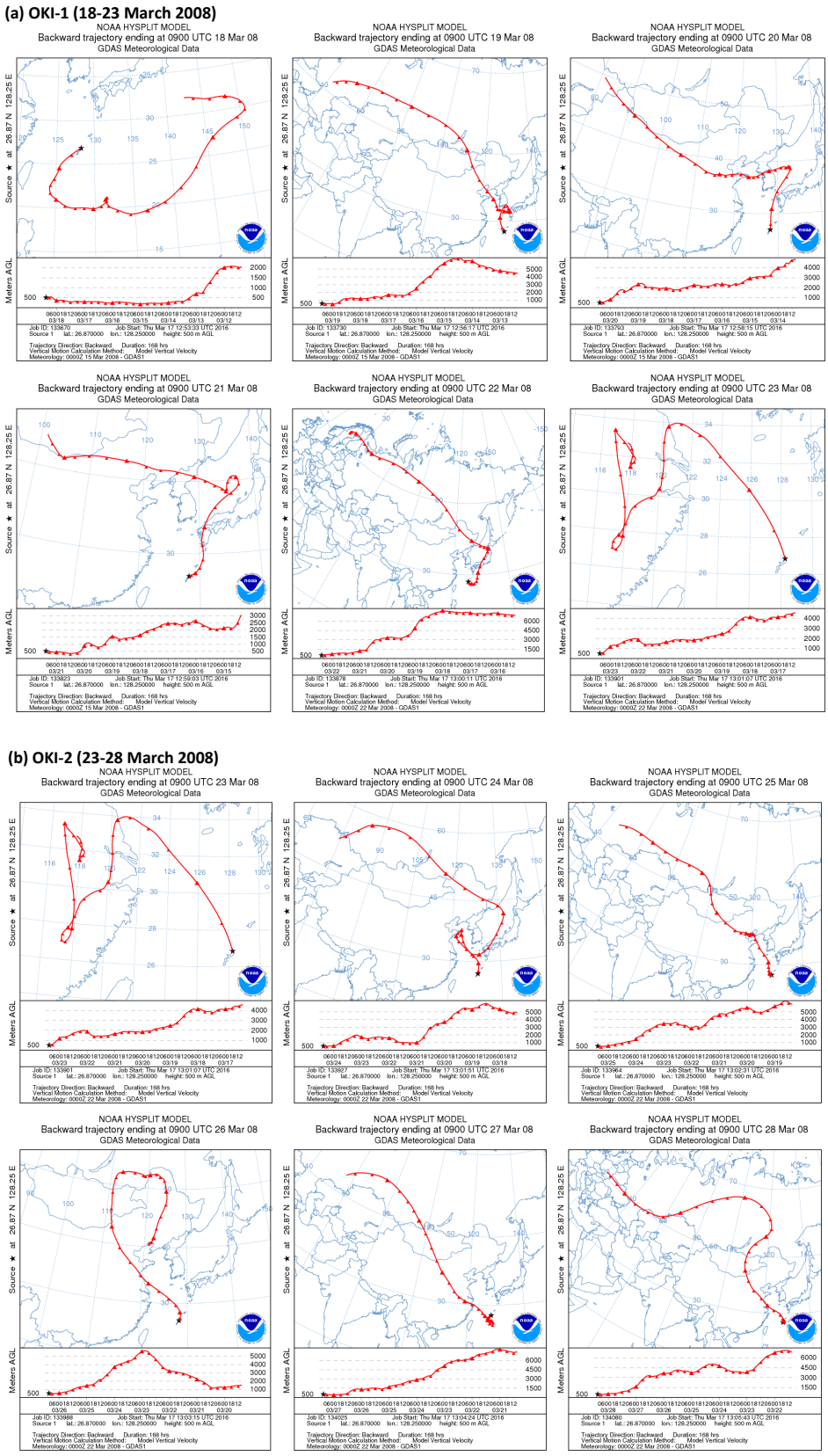

Figure S1. Seven-day backward air mass trajectories (NOAA HYSPLIT) at 500 m a.g.l. corresponding to 0900 UTC for the aerosol samples collected (OKI-1 to OKI-5) in Okinawa Island. The dates along with the sample ID are the starting and ending times for the collection of aerosol samples in Okinawa Island.

Figure S1 continue..

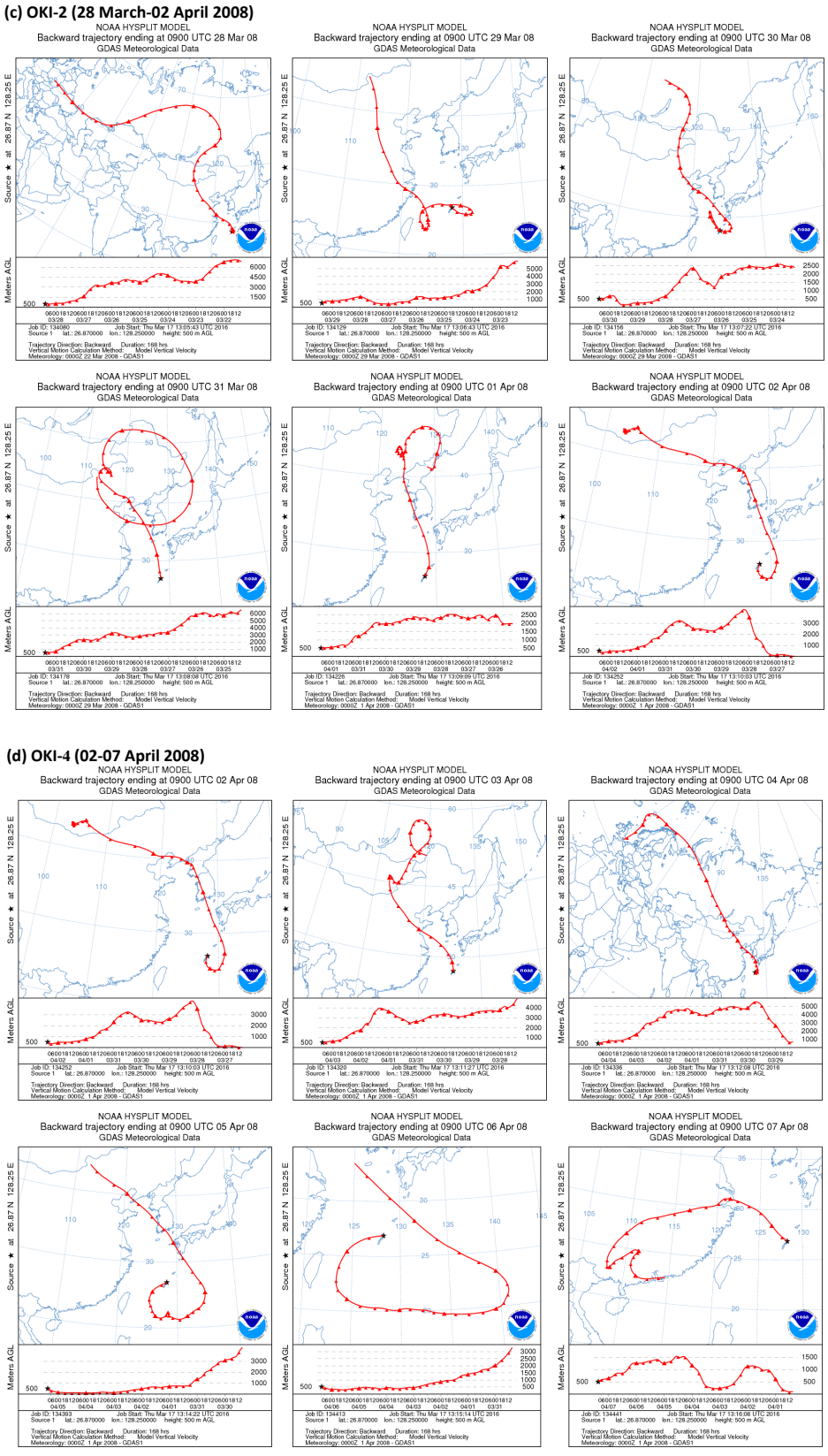

Figure S1 continue..

(e) OKI-5 (10-13 April 2008)

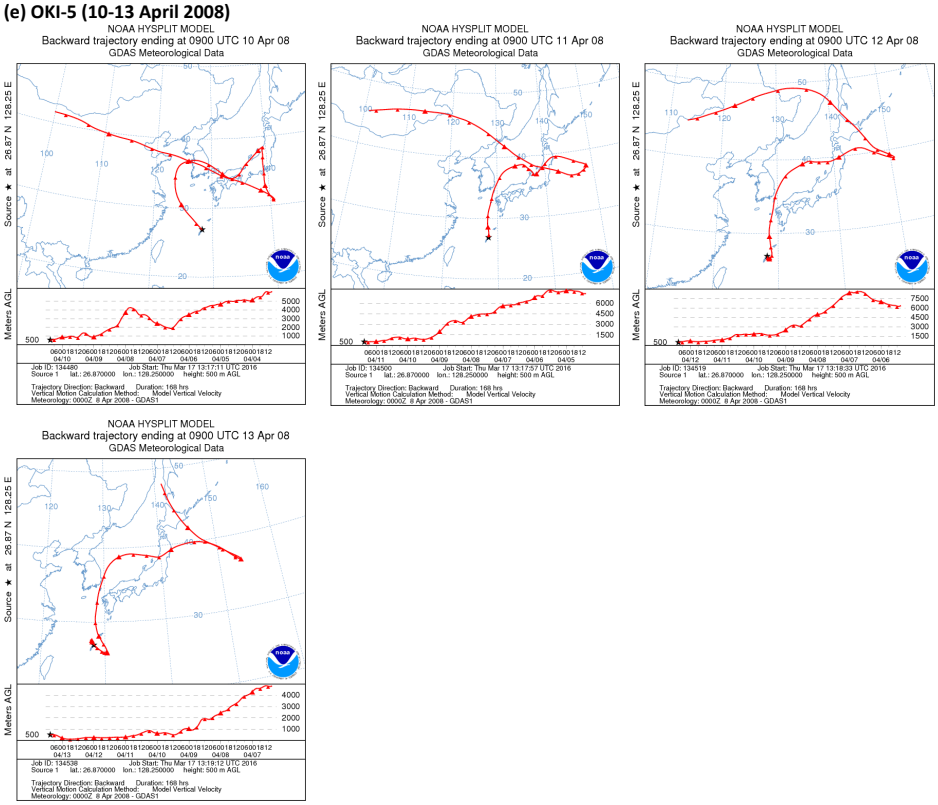

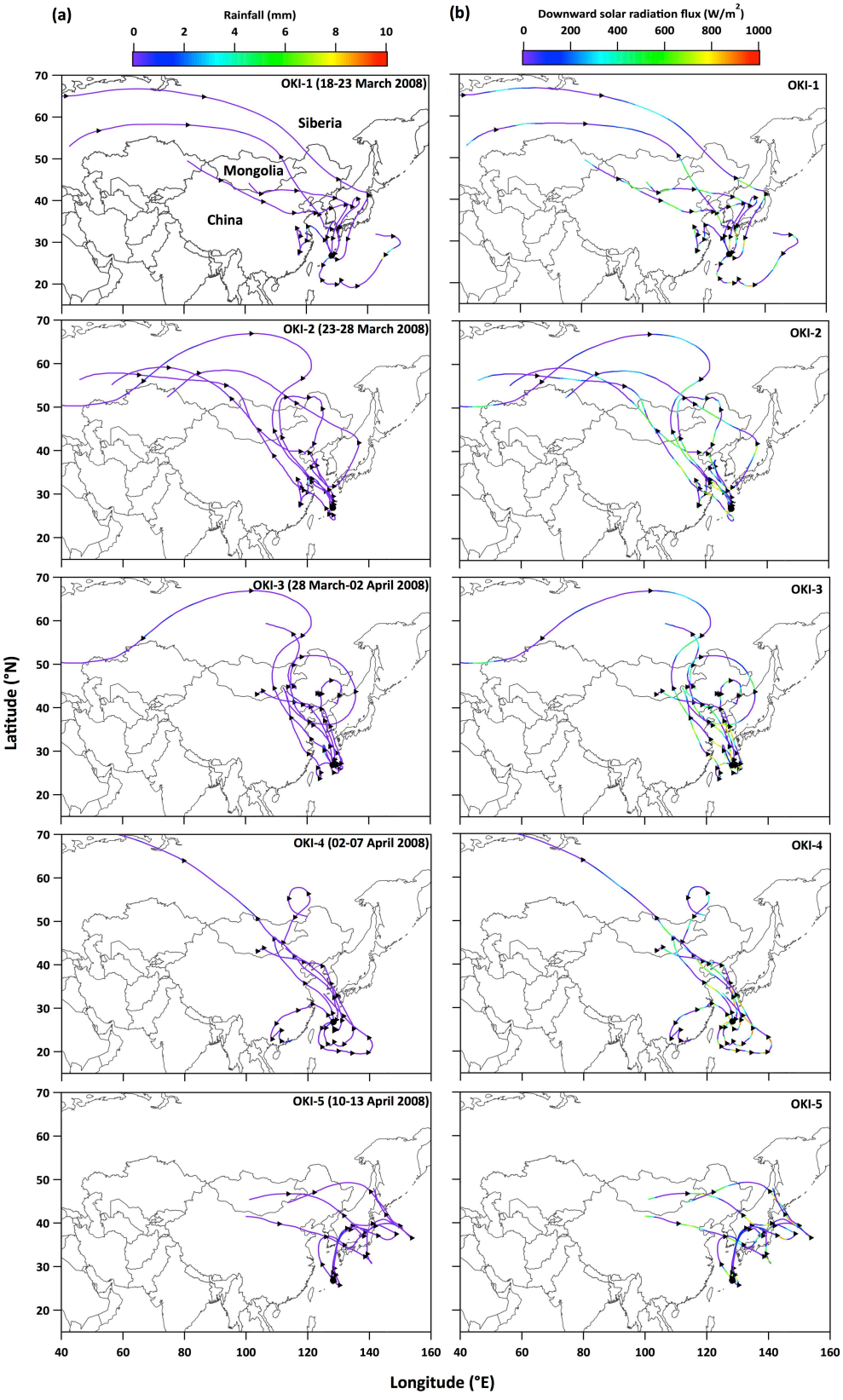

Figure S2. Seven-day backward air mass trajectories (NOAA HYSPLIT) at 500 m a.g.l. (0900 UTC) along with the data of (a) precipitation and (b) downward solar radiation flux for the aerosol samples collected (OKI-1 to OKI-5) in Okinawa Island. The dates given in each panel in figure are the starting and ending times of collection of aerosol samples in Okinawa Island.

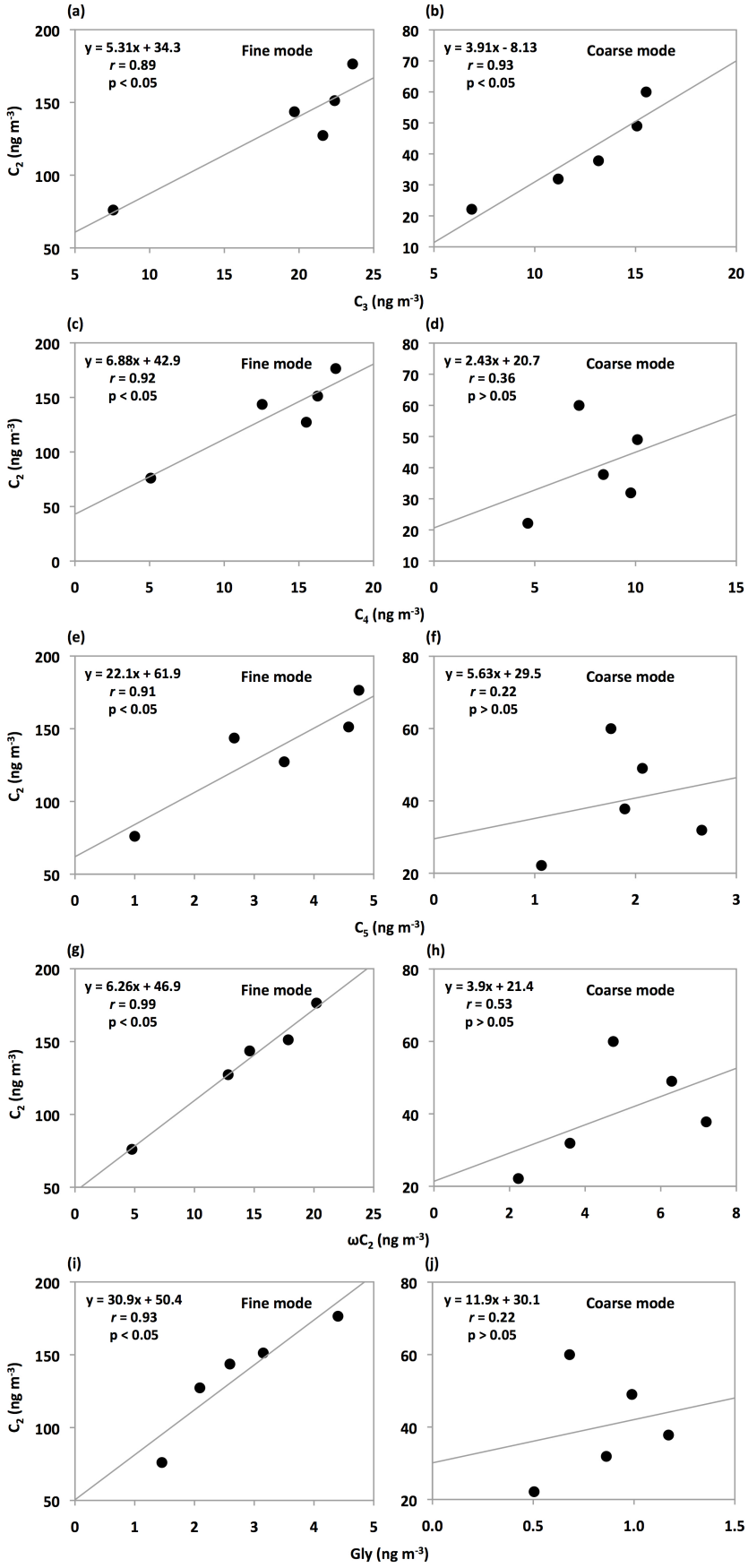

Figure S3. The scatter plots of C_2 with C_3-C_5 diacids, ωC_2 and Gly in fine and coarse mode aerosols in Okinawa.

Table S1. Correlation coefficient (r) and slope of the linear regression of oxalic acid (C_2) with other diacids and related compounds together with their statistical significance between fine and coarse mode aerosols in Okinawa Island.

Linear regression	Fine mode		Coarse mode						
	Correlation coefficient (r)	Slope	Correlation coefficient (r)	Slope	t-score	p-value	df	t-critical at p = 0.05	Slope significance*
C_2 vs. C_3	0.89	5.31	0.93	3.91	0.92	>0.05	6	2.45	Not significant
C_2 vs. C_4	0.92	6.88	0.36	2.43	1.12	>0.05	6	2.45	Not significant
C_2 vs. C_5	0.91	22.1	0.22	5.63	2.61	<0.05	6	2.45	Significant
C_2 vs. ωC_2	0.99	6.26	0.53	3.90	0.65	>0.05	6	2.45	Not significant
C_2 vs. Gly	0.93	30.9	0.22	11.9	2.53	<0.05	6	2.45	Significant

See Table 2 for abbreviation.
df = degree of freedom.
*If, t-score > t-critical => reject null hypothesis => difference in the slope is significant.

Table S2. Correlation coefficient (r) and slope of the linear regression of oxalic acid (C_2) with other diacids and related compounds together with their statistical significance in fine mode aerosols in Okinawa Island.

Linear regression	Correlation coefficient (r)	Slope	Linear regression	Correlation coefficient (r)	Slope	t-score	p-value	df	t-critical at p = 0.05	Slope significance*
C_2 vs. C_3	0.89	5.31	C_2 vs. C_4	0.92	6.88	0.73	>0.05	6	2.45	Not significant
C_2 vs. C_3	0.89	5.31	C_2 vs. C_5	0.91	22.1	2.83	<0.05	6	2.45	Significant
C_2 vs. C_4	0.92	6.88	C_2 vs. C_5	0.91	22.1	2.51	<0.05	6	2.45	Significant
C_2 vs. ωC_2	0.99	6.26	C_2 vs. Gly	0.93	30.9	3.36	<0.05	6	2.45	Significant

See Table 2 for abbreviation.
df = degree of freedom.
*If, t-score > t-critical => reject null hypothesis => difference in the slope is significant.